npj | flexible electronics

www.nature.com/npjflexelectron

REVIEW ARTICLE OPEN

Check for updates

Wearable, epidermal devices for assessment of swallowing function

Tarek Rafeedi[1], Abdulhameed Abdal[2], Beril Polat[1], Katherine A. Hutcheson[3], Eileen H. Shinn[4] and Darren J. Lipomi[1]✉

Swallowing is an ensemble of voluntary and autonomic processes key to maintaining our body's homeostatic balance. Abnormal swallowing (dysphagia) can cause dehydration, malnutrition, aspiration pneumonia, weight loss, anxiety, or even mortality—especially in older adults—by airway obstruction. To prevent or mitigate these outcomes, it is imperative to regularly assess swallowing ability in those who are at risk of developing dysphagia and those already diagnosed with it. However, current diagnostic tools such as endoscopy, manometry, and videofluoroscopy require access to clinical experts to interpret the results. These results are often sampled from a limited examination timeframe of swallowing activity in a controlled environment. Additionally, there is some risk of periprocedural complications associated with these methods. In contrast, the field of epidermal sensors is finding non-invasive and minimally obtrusive ways to examine swallowing function and dysfunction. In this review, we summarize the current state of wearable devices that are aimed at monitoring swallowing function and detecting its abnormalities. We pay particular attention to the materials and design parameters that enable their operation. We examine a compilation of both proof-of-concept studies (which focus mainly on the engineering of the device) and studies whose aims are biomedical (which may involve larger cohorts of subjects, including patients). Furthermore, we briefly discuss the methods of signal acquisition and device assessment in relevant wearable sensors. Finally, we examine the need to increase adherence and engagement of patients with such devices and discuss enhancements to the design of such epidermal sensors that may encourage greater enthusiasm for at-home and long-term monitoring.

npj Flexible Electronics (2023)7:52 ; https://doi.org/10.1038/s41528-023-00286-9

INTRODUCTION

Swallowing—deglutition—is a physiological process where the muscles of the mouth, throat, and esophagus pass a portion of food or liquid from the oral cavity to the stomach in a coordinated sequence. The process starts with a voluntary initiation and continues with a series of involuntary actions of the muscles[1]. The stages of swallowing and their mechanics are described by paradigmatic models[2,3]. These models, such as four stage (for liquid) and process models (for solids), describe the role of relevant anatomical structures chronologically organized by the bolus passage from the oral cavity to the esophagus. In dysphagia (abnormal swallowing) assessment, the models help examine the abnormalities in bolus movement and airway protection to aid in the diagnosis and therapy. Dysphagia can be caused by obstructive and damaged tissue from injury, surgical complications, or muscular damage, especially in old age or myopathic disorders[4–8]. It can also be of neurological origins; characterized by impaired control of the peripheral structures that are critical in regulating muscle coordination for swallowing activity[9]. Reduction in nerve conduction, for instance, may lead to elongated timing of swallowing events[10–13]. Incidentally, this disease can be caused by or correlated with neurological ailments such as strokes, Parkinson's disease, and dementia, as well as autoimmune diseases such as scleroderma[5,14,15]. The underlying origin of the disease calls for different diagnostic techniques and different courses of treatment. A recent systematic review and meta-analysis showed that the global prevalence of oropharyngeal dysphagia follows an increasing trend[16]. In the United States, a 2018 study found that 16.1% of the population described having dysphagia[17]. Other studies suggest that dysphagia occurs in 8–22% of populations over 50 years old, and the number is generally higher for nursing home residents[18,19].

Although dysphagia can be managed and rehabilitated by interdisciplinary providers including otolaryngologists, gastroenterologists, and speech-language pathologists, it is often a chronic condition requiring lifelong care[4,20–22]. Procedural and pharmacologic mitigation strategies, as well as a range of exercise maneuvers, have been utilized to curb the development and treat this condition[23–32]. However, complete recovery from swallowing impairment is often elusive even with successful management[33,34]. If insufficiently addressed, degraded swallowing function may lead to aspiration pneumonia, weight loss, and anxiety over nutritional intake[35–37]. To diagnose this condition clinicians use tools such as videofluorscopy[38–40], endoscopy[41–43], and high-resolution manometry[44,45]. These tools and procedures are all exclusive to clinical, often specialized, settings, which reduces the access of at-risk populations (e.g., poor, rural, or elderly). Access is further diminished by the cost and the necessity of experienced technicians/clinicians to operate these devices. Additionally, clinical procedures may also cause periprocedural complications, such as pain, injury, and/or anxiety in the case of endoscopy, and risks associated with X-ray exposure in the case of videofluoroscopy[44]. Further, in-clinic screening protocols for swallowing and aspiration such as the Mann Assessment of Swallowing Ability (MASA), Water-swallow Test (WST), Gugging Swallow Screen

[1]Department of NanoEngineering, University of California, San Diego 9500 Gilman Drive, Mail Code 0448, La Jolla, CA 92093-0448, USA. [2]Department of Mechanical and Aerospace Engineering, University of California, San Diego 9500 Gilman Drive, Mail Code 0448, La Jolla, CA 92093-0448, USA. [3]Department of Head and Neck Surgery, Division of Surgery, Division of Radiation Oncology, The University of Texas MD Anderson Cancer Center, Unit 1445, 1515 Holcombe Street, Houston, TX 77030-4009, USA. [4]Department of Behavioral Sciences, The University of Texas MD Anderson Cancer Center, Unit 1330, 1155 Pressler Street, Houston, TX 77230-1439, USA. ✉email: dlipomi@ucsd.edu

(GUSS), and their variations, require the administration and expertise of a trained clinician[46–49].

Limitations of the current clinical procedures coupled with the opportunities to measure swallowing activity in the natural environment (outside of clinical settings) led researchers to examine different diagnostic tools that are less invasive and unobtrusive. Recent work in skin-interfacing ("epidermal") electronic devices[50–53] promises to increase access and increase the temporal resolution of measurements (since they can be done between visits to the clinic) with the potential to decrease healthcare costs, inconvenience, and procedural anxiety. Ideally, incorporating advances in nanomaterial-enabled sensors, biomechanics, and machine learning could lead to a role for epidermal devices in the monitoring and rehabilitation of diseases such as dysphagia.

In this review, we briefly introduce the physiological structures and biomechanical stages involved in swallowing. After this, we present a detailed overview of recent innovations within the field of skin-interfacing wearable sensing modalities utilized for detecting and monitoring swallowing, primarily in the oropharyngeal stages (see Fig. 1). Within each sensing modality, we highlight a few of the materials utilized (summarized in Table 1) and discuss their functional physical properties. Finally, we probe the challenges and opportunities to transitioning these materials-enabled sensors to an impactful tool for in-clinic and out-of-clinic (at-home) care.

Swallowing physiology

Physiologically, a swallow is initiated with a voluntary act and sustained with the precise coordination of more than 30 pairs of muscles[1,54]. The activity recruits different layers of the central nervous system from the cerebral cortex to the medulla oblongata[55]. Swallowing involves many anatomical structures starting with the oral cavity, pharynx, larynx, and esophagus[2,56,57]. Along with these structures, other muscles, bones, cartilage, and salivary glands work in coordination to propel the bolus from the oral cavity to the esophagus. Physiologically, swallowing is described differently for liquid and solid boluses. For instance, in describing swallowing liquids, the four-stage model is generally used, whereas for swallowing solids, the process model may be followed[3,58,59].

The four-stage model as shown in Fig. 1b consists of four distinct phases. The first phase is called the oral preparatory stage, and it starts as a bolus is taken into the mouth. The bolus is held on the tongue surface while the anterior and posterior parts of the oral cavity are sealed to prevent leakage into the oropharynx. The tongue propels the bolus from the anterior oral cavity through the posterior into the pharynx in a process known as the oral propulsive stage. The pharyngeal and oral propulsive stages tend to rapidly transition for liquid swallows. In the case of solid boluses, the process model delineates the events before the swallow enters the pharyngeal stage[2,60]. After ingestion of the solid, stage transport occurs when the tongue carries the bolus to the post-canine region onto the lower teeth for chewing. During mastication, cyclic movement of the jaw is established with the coordination of the tongue, cheek, soft-palate, and hyoid bone[3,61]. As opposed to liquid swallows, the posterior oral cavity is not thoroughly sealed during this phase[62,63]. Although mastication and the motion of solid boluses within the oral cavity are vital to the execution of the swallow, they go beyond the scope of this review as they bring into question oral, dental, and mandibular assessments among other matters.

Common to liquids and solids, the pharyngeal stage characterizes the propulsion of the bolus through the pharynx into the esophagus (see Fig. 1a, b). Tight air compression results in pressure on the bolus to achieve clearance through the upper aerodigestive tract[64]. With the elevation of the soft-palate and tongue base retraction, the bolus is pushed against the pharyngeal walls and squeezed downstream. To protect the airways, the vocal folds are closed to seal the glottis[65,66]. The arytenoids tilt forward to contact with the epiglottic base while the hyoid bone and larynx are pulled upward by the contraction of the suprahyoid muscles and thyrohyoid muscles tilting the epiglottis backward. This sequence seals the laryngeal vestibule as the upper esophageal sphincter relaxes and expands to allow the bolus to pass into the esophagus[67–69]. The esophageal stage transits the intake to the lower esophageal sphincter, and eventually into the stomach by peristalsis.

Clinical diagnostic tools

Standardized diagnostic tools such as X-ray videofluoroscopy require the patient to swallow a series of radiocontrast agents (e.g., barium sulfate). These agents can have various viscosities and allow for real-time visualization and assessment of swallowing mechanics. Direct visualization supports the assessment of bolus clearance, including abnormalities such as laryngeal penetration/aspiration and residue (see Fig. 1c). It is however accompanied by minor risk factors, namely exposure to ionizing radiation, and/or dulling of taste intensity[70] and rare allergic reactions[71,72] due to exposure to barium. A more quantitative examination of pharyngeal and upper esophageal sphincter functional abnormalities can be done using high-resolution manometry, to measure internal pressures caused by muscular exertions[70]. This technique uses a manometric catheter containing several circumferential pressure sensors targeting a series of anatomical structures (e.g., from the velopharynx down to the upper esophageal sphincter). These measurements provide localized pressure evaluation and insight into the timing and coordination of the swallow as seen in Fig. 1d[45]. Although it is more quantitative, manometry still requires evaluation by a trained clinician and is minimally invasive by the nature of transnasal insertion of a catheter. In contrast, wearable sensors cannot produce visualizations such as those shown in Fig. 1c, nor capture the internal pressure of manometry; however, they can offer less obtrusive sensing of swallow exertions and correlated respiratory activity[64,73–75].

Assessment of electromyographic (EMG) activity, superficially or intramuscularly, is currently considered a non- or minimally invasive tool for assessing muscle function or providing biofeedback in swallow disorder therapy[76,77]. The muscle groups that are frequently probed include the jaw and perioral, submandibular, tongue, laryngeal and pharyngeal, and cricopharyngeal muscle of the upper esophageal sphincter[55]. The biopotentials activity of the former two groups is measurable by surface electromyography (sEMG), due to their proximity to the skin. Therefore, sEMG has its limitations when targeting deeper muscle groups. The rest are approached with needle EMG electrodes for deeper and localized targeting, either via the skin or endoscopically, which are currently irreplaceable. The potential risks such as hematoma and pain during coughing, and the precision required for placement constrain the applicability of needle electrodes to clinical settings[69,78]. Although EMG has some clinical applications, it is not typically used in the diagnosis of swallow disorders. The neuromuscular signals extracted from electromyographic activity, however, can help detect swallowing abnormalities especially when combined with orthogonal forms of sensing and adequate data analysis techniques.

Wearable sensing modalities for swallowing behavior

Surface electromyography electrodes. Biopotential signals are the sum of action potentials fired by excitable cells such as neurons, myocytes, and cardiomyocytes. They are generated from changes in ion concentration through depolarization and repolarization of the cell membrane, manifesting in the extracellular fluid. Skeletal muscle activity generates such signals. Motor nerve pulses cause

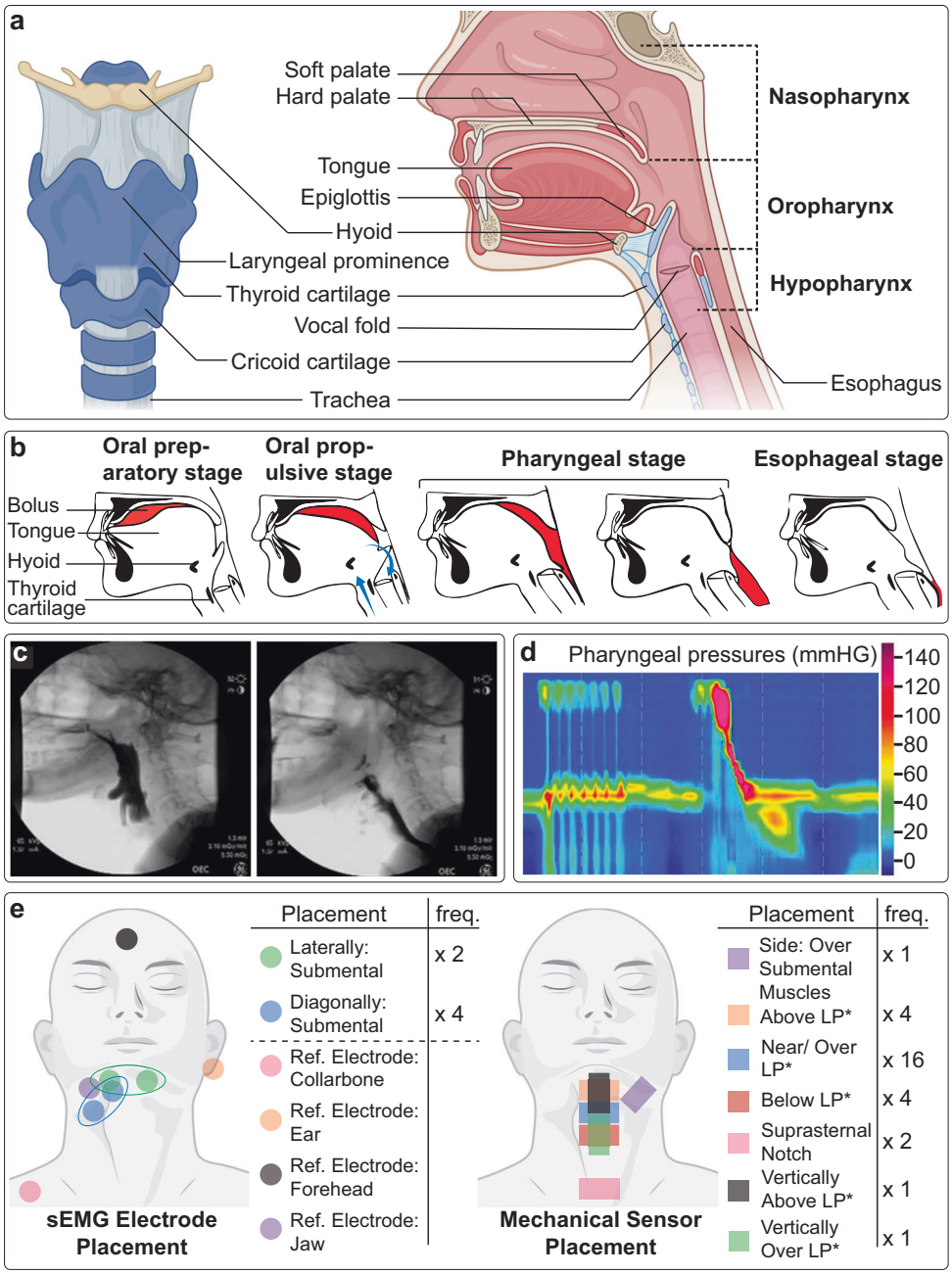

Fig. 1 Illustrates the physiology and anatomy relevant to swallowing and its characterization. a Depicts a sagittal cross-section of the oral to upper esophageal anatomy of the digestive tract (*right*) and a frontal plane depiction of the larynx (*left*) highlighting relevant anatomies. **b** Is a recreated figure showing the phases of the four-stage model for liquid swallowing (arrows were added to depict larynx and epiglottis motion). **c** Images of dysphagic videofluorscopy swallows showing penetration into the vocal folds *(left)* and aspiration *(right)*. **d** A graphical representation of high-resolution manometry results with initial velopharyngeal vocalizations where the horizontal axis is time, the vertical is the relative location and the color scheme represents pressure. **e** A schematic depicting the visually examined placement of materials-enabled sEMG sensing electrodes *(left)* and proximal placements of the reference electrode, and mechanical sensors *(right)* with flexible or stretchable characteristics used in recent literature. The number of electrodes/sensors with similar placement (freq.) is shown in the tables adjacent to each panel. **Note LP: Laryngeal prominence*. Panel **b** and **c** reproduced with permission[2,70].

muscle fibers to discharge creating motor unit action potentials that compose an EMG signal[79,80]. A differential voltage can be measured from a pair of electrodes to reveal the depolarization and repolarization phases caused by muscle contraction and relaxation. Such signals can be obtained from epidermal electrodes placed over the target muscle(s). The electrodes convert the propagated ionic currents from muscle activity into the electric current at the electrode interface. The collected electrophysiological signal can later be processed to extract frequency and amplitude features for determining the timing, force, and fatigue of the muscle. The capabilities of such epidermal electrodes have been applied to digitalized medical devices for tremor diagnosis, muscle rehabilitation, gait assessment, and detection of bruxism, among other applications[81–85].

To collect these sEMG signals with high quality, strong electrical contact is needed between the electrode and skin. Commercially available Ag/AgCl electrodes use a thick layer of ionic gel to maintain a contact low impedance between the metal electrode

Table 1. A categorical summary of epidermal swallow sensors enabled by recent developments in stretchable conductors and materials.

Sensing modality	Source	Year	Sensor location	Active materials	SNR	GF/sensitivity	Spatial resolution	Human subject experiments	Wireless (y/n)	Sensing mechanism
EMG	Constantinescu et al., *Med. Eng. Phys*., 38, 807–812	2016	Side (right) of the chin (targeting the right anterior belly of the digastric muscle)	200 nm Au	6.138	-	One pair of sEMG sensor	Proof-of-concept	N	Biopotential
	Nicholls et al., *Second IEEE PerCom Workshop on Pervasive Health Technologies*, 413–418	2017	Side (left) along submental muscles	300 nm Au	21.4	-	One pair of sEMG sensor	Proof-of-concept	Y	Biopotential
	Lee et al., *Sci. Rep*. 7, 1–12	2017	Laterally across submental muscles	300 nm thick gold	21.4	-	One pair of sEMG sensor	Proof-of-concept	Y	Biopotential
	Kim et al., *Sci. Adv*. 5, 1–10	2019	Sides (left and right) along submental muscles	9 μm Cu and 500 nm Au	-	-	Two pairs of sEMG sensors and a strain sensor	Proof-of-concept	Y	Biopotential
	Kantarcigil et al., *J. Speech, Lang. Hear. Res*. 63, 3293–3310	2020	Sides (left and right) along submental muscles	9 μm Cu and 500 nm Au	20.64	-	Two pairs of sEMG sensors	Cohort study	Y	Biopotential
	Polat et al., *Adv. Sensor Res*. 2200060	2023	Laterally across submental muscles	PEDOT:PSS(1)-b-PPEGMEA(6)	-	-	One pair of sEMG sensor	Cohort study	Y	Biopotential
	Wang et al. *Sci. Adv*. 6: eabd0996	2020	Multi electrode array placed on the neck and upper chest	100 nm Au	-	-	16 channel sEMG patch	Proof-of-concept	N	Biopotential
Strain	Roh et al., *ACS Nano* 9, 6252–6261	2015	Medially and horizontally near laryngeal prominence (by inspection)	SWCNTs embedded in PEDOT:PSS/PU complex	-	~136.7 for 2.1% strain	One strain sensor	Proof-of-concept	N	Piezoresistive
	Hwang et al., *ACS Nano* 9, 8801–8810	2015	Medially and horizontally near laryngeal prominence (by inspection)	AgNWs embedded in PEDOT:PSS/PU complex	-	~12.4 for 2% strain; ~1 for 10–60%	One strain sensor	Proof-of-concept	N	Piezoresistive
	Zhu et al., New J. Chem. 41, 4950–4958	2017	Medially and horizontally near laryngeal prominence (by inspection)	CuNWs and WGPs	-	~175,000 for 2.5% strain	One strain sensor	Proof-of-concept	N	Piezoresistive
	Ramirez et al., *ACS Nano* 12, 5913–5922	2018	Horizontally side submental muscles	PdNIs on graphene	-	~1 for 0.02% strain	One pair of sEMG sensor and one strain sensor	Cohort study	N	Piezoresistive
	Polat et al., *ACS Appl*. Nano Mater. 4, 8126–8134	2021	Medially and horizontally near laryngeal prominence	AuNIs/graphene/ PEDOT:PSS("dough")	-	~17.5 for 0.001% strain	One pair of sEMG sensor and one strain sensor	Proof-of-concept	N	Piezoresistive
	Huang et al., *Smart Mater. Struct*. 27,	2018	Medially and horizontally below laryngeal prominence (by inspection)	GNPs and CB/SWCNTs	-	~2 for 2.5% strain	One strain sensor	Proof-of-concept	N	Piezoresistive

Table 1 continued

Sensing modality	Source	Year	Sensor location	Active materials	SNR	GF/sensitivity	Spatial resolution	Human subject experiments	Wireless (y/n)	Sensing mechanism
	Zang et al., *Biomed. Phys. Eng. Express* 5,	2019	Medially and horizontally near laryngeal prominence (by inspection)	RGO	-	~250 for 2.5% strain	One strain sensor	Proof-of-concept	N	Piezoresistive
	Zhang et al., *Sensors (Switzerland)* 17, 1–10	2017	(Unclear)	([EMIM][TFSI]) as the ionic liquid (IL)	-	~560 for 2% strain	One strain sensor	Proof-of-concept	N	Piezoresistive
	Sun et al., *Chem. Eng. J.* 382, 122832	2020	Medially and horizontally above laryngeal prominence (by inspection)	PAAm-oxCNTs	-	1.5 between 0–250% strain range	One strain sensor	Proof-of-concept	N	Piezoresistive
	Wang et al., *J. Mater. Chem.* C 9, 575–583	2021	Medially and horizontally near laryngeal prominence (by inspection)	PANI/ANF-PVA	-	~40 for 5% strain	One strain sensor	Proof-of-concept	N	Piezoresistive
	Xu et al., *Colloids Surfaces A Physicochem. Eng. Asp.* 636, 128182	2022	Medially and horizontally below laryngeal prominence (by inspection)	MXene nanosheets	-	3.2 between 50–300% strain	One strain sensor	Proof-of-concept	N	Piezoresistive
	Joeng et al. *NPG Asia Materials* 9, e443	2017	Medially near laryngeal prominence (by inspection)	Encapsulated liquid GaInSn	-	2 for ~30% strain	One strain sensor	Proof-of-concept	Y	Piezoresistive
	Wang et al., *Adv. Funct. Mater.*	2021	Medially and vertically over laryngeal prominence (by inspection)	RGO and CNT	-	7.2 for 0–60% strain; 89 for 60-120%	One strain sensor	Proof-of-concept	N	Piezoresistive
	Kim et al., *Sci. Adv.* 5, 1–10	2019	Medially and vertically above laryngeal prominence (by inspection)	Patterened Velostat, 3 M	-		Two pairs of sEMG and one strain sensor	Proof-of-concept	Y	Piezoresistive
	Polat et al., *Adv. Sensor Res.* 2200060	2023	Medially and horizontally near laryngeal prominence	AuNIs/graphene/ PEDOT:PSS("dough")	-	~17.5 for 0.001% strain	One pair of sEMG sensor and one strain sensor	Cohort Study	Y	Piezoresistive
	Zhang et al. *Adv. Electron. Mater.* 5, 1900285	2019	Medially and horizontally near laryngeal prominence (by inspection)	MXene/ PVA Hydrogel	-	~0.4 for 200% strain	One strain sensor	Proof-of-concept	N	Capacitive
Pressure	Kou et al., *Sci. Rep.* 9, 1–7	2019	Medially near laryngeal prominence (by inspection)	NH4HCO3/Gr	-	0.12 kPa^{-1} between 0–10 kPA	One pressure sensor	Proof-of-concept	Y	Capacitive
	Xia et al., *Adv. Mater. Technol.* 5, 1–8	2020	Medially below laryngeal prominence (by inspection)	NIPAm/Bis/AAc	-	10.1 kPa^{-1} for 2–40 Pa and 1.1 kPa^{-1} for 40–110 Pa	One pressure sensor	Proof-of-concept	Y	Capacitive
	Maeda et al., *IEEE 3rd Glob. Conf. Life Sci. Technol.* 315–316	2021	Medially near laryngeal prominence	Hetero-core fiber optic	-	-	One pressure sensor	Proof-of-concept	N	Optical

Table 1 continued

Sensing modality	Source	Year	Sensor location	Active materials	SNR	GF/sensitivity	Spatial resolution	Human subject experiments	Wireless (y/n)	Sensing mechanism
	Iizuka et al., *J. Physiol. Sci.* 68, 837–846	2018	Medially above (0.5-1.0 cm) the laryngeal prominence	PVDF	~75-100	-	Five pressure sensors	Proof-of-concept	N	Piezoelectric
	Natta el., *ACS Sensors* 6, 1761–1769	2021	Medially above laryngeal prominence (by inspection)	AlN	-	0.025 V/N	One pair of sEMG sensors and one pressure sensor	Cohort study	Y	Piezoelectric
	Lee et al., *Polymers (Basel)*. 13	2021	Medially near laryngeal prominence (by inspection)	Au(Phen)Cl2+ ion with Au	-	1.5 x e^-6 mV/kPa	One pressure sensor	Proof-of-concept	N	Ionic polymer–metal composite
	Guan et al.	2021	Medially near laryngeal prominence (by inspection)	MoSe2/MWNT		0.24-0.35 kPa-1	One pressure sensor	Proof-of-concept	N	Piezoresistive
	Park et al. *Adv. Mater*. 29, 1702308	2017	Medially below laryngeal prominence (by inspection)	PZT		0.018 kPa−1	One pressure sensor	Proof-of-concept	Y	Piezoelectric
Mechano-acoustic	Tao et al., *Nat. Commun*. 8, 1–8	2017	Medially near laryngeal prominence	Laser-induced graphene	-	31 mV/Pa	One acoustic sensor	Proof-of-concept	N	Resistance
	Lee et al., *Nat. Biomed. Eng*. 4, 148–158	2020	Over suprasternal notch	N/A	-	-	One IMU sensor	Cohort study	Y	Motion/ Acceleration
	Kang et al. *NPJ Digital Med*.	2022	Over suprasternal notch/over laryngeal prominence	N/A	-	-	Two IMU Sensors	Cohort study	Y	Motion/ Acceleration

and the skin (hence referred to as wet electrodes). Dry electrodes, on the other hand, require direct and intimate contact between the conductor and the skin. For a better understanding of this electrical contact, resistor-capacitor circuit models are used to design and characterize such electrodes. The Cole bioimpedance model is commonly used for the skin, while electrode models depend on their type and geometry[86,87]. For instance, in a dry electrode, the top layer of the stratum corneum (~800 nm thickness) is considered as the dielectric material quantifying the capacitance (C_{SC}) of the circuit. Whereas in gel electrodes, the double-layer capacitance (C_{DL}) of the electrolyte gel is utilized[88]. Figure 2a shows the skin and electrode interface of typical wet and dry electrodes and the dry electrode equivalent circuit model in Fig. 2b. Recent advancements in thin film and compliant conductive materials and geometries have popularized research on dry electrodes producing compact and unobtrusive wearable electrodes.

Action potentials propagated from the deep skin layers can attenuate at the top surface of the skin due to the insulative nature of the stratum corneum (mainly consisting of dead corneocytes)[89]. Thus, the electrode-skin interface is crucial in probing these potentials. Conventional electrodes such as silver/silver-chloride (Ag/AgCl) gel are commercially available and widely used for monitoring muscle activity (among other biopotential activity) because of their reversible electrochemical characteristics. Typical electrolyte gel disperses on the human skin to maintain stable electrical properties between the electrode and skin interface. Ionic diffusion between Ag^+ and Cl^- ions within the electrolyte gel promotes reversible reactions on the electrode surface. Low polarization potential within the capacitive interface mitigates signal fluctuation and maintains a low impedance with a high signal-to-noise ratio (SNR). Despite their reversibility, long-term monitoring is hindered by the hydration state of the gel, reducing the consistency of the signal measured. Moreover, the thickness and rigidity of typical Ag/AgCl electrodes (Fig. 2a) decrease the expected usability and comfort for continuous monitoring[90].

In swallowing assessment using sEMG, the adequate surface placement of the electrodes on the neck is imperative to capture the pertinent signals while reducing crosstalk from adjacent muscle activity[80]. Several recommendations have been suggested to monitor either suprahyoid or infrahyoid muscle coordination for swallowing, such as placing the electrode couples a few centimeters laterally to the neck midline[79,91]. Other placements include aligning the electrodes with the anterior belly muscle fibers[75,92]. This is located over the gap between thyroid and cricoid cartilages (see Fig. 1a, e). Moreover, the submental surface is an area of interest to monitor the suprahyoid muscle group, which affects hyoid excursion and the opening of the upper esophageal sphincter[79,93]. In these locations, electrodes can experience frequent mechanical stress exerted by swallowing and neck motion, not to mention the effect of perspiration and body heat on their adhesiveness. Therefore, for longer-term wearable monitoring, better compliant and durable electrodes are required for such applications. Electrode placements observed in recent literature on conformal electrode designs for swallowing are summarized in Fig. 1e *(left)*. While all these placements are capable of capturing the occurrence of the swallow, further investigation is needed to understand the effect of placement on dysphagia detection and estimations of bolus volume. Previous studies utilizing sEMG have statistically examined the effects of bolus viscosity, volume, and participant age on muscle activation patterns[94,95].

The benefits of a conductive medium such as a gel or paste as a junction between the skin and electrode material have led researchers to examine wet electrode materials based on polymer hydrogels. These cross-linked polymer networks retain the electrolyte solution and can be made using biocompatible precursors and rendered mechanically soft and self-adhesive. They can maintain robust contact with biological substrates and maintain signal fidelity without requiring rigid carrier substrates[96–98]. Although hydrogel bioelectronics is exceptionally versatile and tunable in properties, dehydration caused by water transport to the environment can influence their long-term performance[99,100]. Increasing the water retention capacity by varying electrolyte concentration can be achieved by adding salts[101,102].

The exceptional electrical conductivities of metals like gold and copper are indispensable in integrated wearable sensors[103]. However, their mechanical stiffness precludes them from conforming and/or adhering to curved anatomical surfaces, hence they require intricate geometric patterning. Serpentine, buckled, or fractal geometries, can deflect incurred mechanical stress to geometric deformation thus increasing the fracture strain of the metal trace (Fig. 2c, d)[51,92,104,105]. To give these electrodes an elastic restoring force, they are fabricated on a thin (~5 µm) layer of elastomer such as polydimethylsiloxane (PDMS). For improved skin adhesion, a bioadhesive backing (such as Silibione) can be added to laminate the electrode on the submental surface[92]. Thin metal electrode features are generally patterned with photolithography and physical vapor deposition and supported with a polyimide layer to minimize the bending stress. Finally, a reactive ion etch is used to expose the electrode windows. The stretchability of the mesh filamentary serpentine electrode (~30%) geometry (seen in Fig. 2d) exceeds the elasticity of the human skin and complements curvilinear boundaries with a radius of curvature of 45 µm. Two of the electrodes in the patch were placed along (and targeted) the anterior belly of the digastric muscle, while the third was used as a ground. The integrated submental ground electrode on the patch showed lower swallow signal amplitudes when compared to the ground placement on the elbow (likely chosen as a control for its distance from the neck), but it showed lower signal sensitivity to head movements. The size restriction imposed by the additive methods of such fabrication procedures reduces the spatial resolution and span of the epidermal sensor, a key factor for more accurate and extensive monitoring[53,106]. In that regard, subtractive (top-down) fabrications can yield larger sensor patches allowing a host of spatial and temporal analyses using ML and statistical analysis[107–109]. Fig. 2g, h shows the spatial mapping achievable with sEMG electrodes and emphasizes the leap in wearability afforded by new fabrication techniques and advancements in materials for epidermal sensing shown in Fig. 2h.

Most sEMG experiments on swallowing behavior have been performed in a laboratory setting. Typically, the wearable sensor is physically tethered to backend electronics. This setup is undesirable for at-home monitoring. To address this issue, wireless data acquisition devices combined with wearable sensors can transmit raw signals to a computer for processing and analysis. Incidentally, skin-like electrodes inspired by fractal gold nano-membranes[110] can incorporate a flexible carbon connector to a wireless transmitter for continuous monitoring with minimal obtrusiveness[111]. Such devices have been employed in a customized biofeedback classification algorithm to engage healthy participants during swallowing experiments. Real-time video game feedback uses the submental muscle activity signal as the controller (thresholds) for a ball bouncing between platforms (Fig. 2f). Cohort studies of the customized human-computer interaction gaming technology were further studied with dysphagic exercises for clinical assessment[112].

Despite the robust electronic properties of metallic thin films, the mechanical mismatch between the materials and the soft skin can introduce electrode motion artifacts—a consequence of interfacial disparities. Additionally, elemental and alloyed metals offer minimal tunability in mechanical and electronic properties in thin films. To that end, conducting polymers such as poly(ethylene

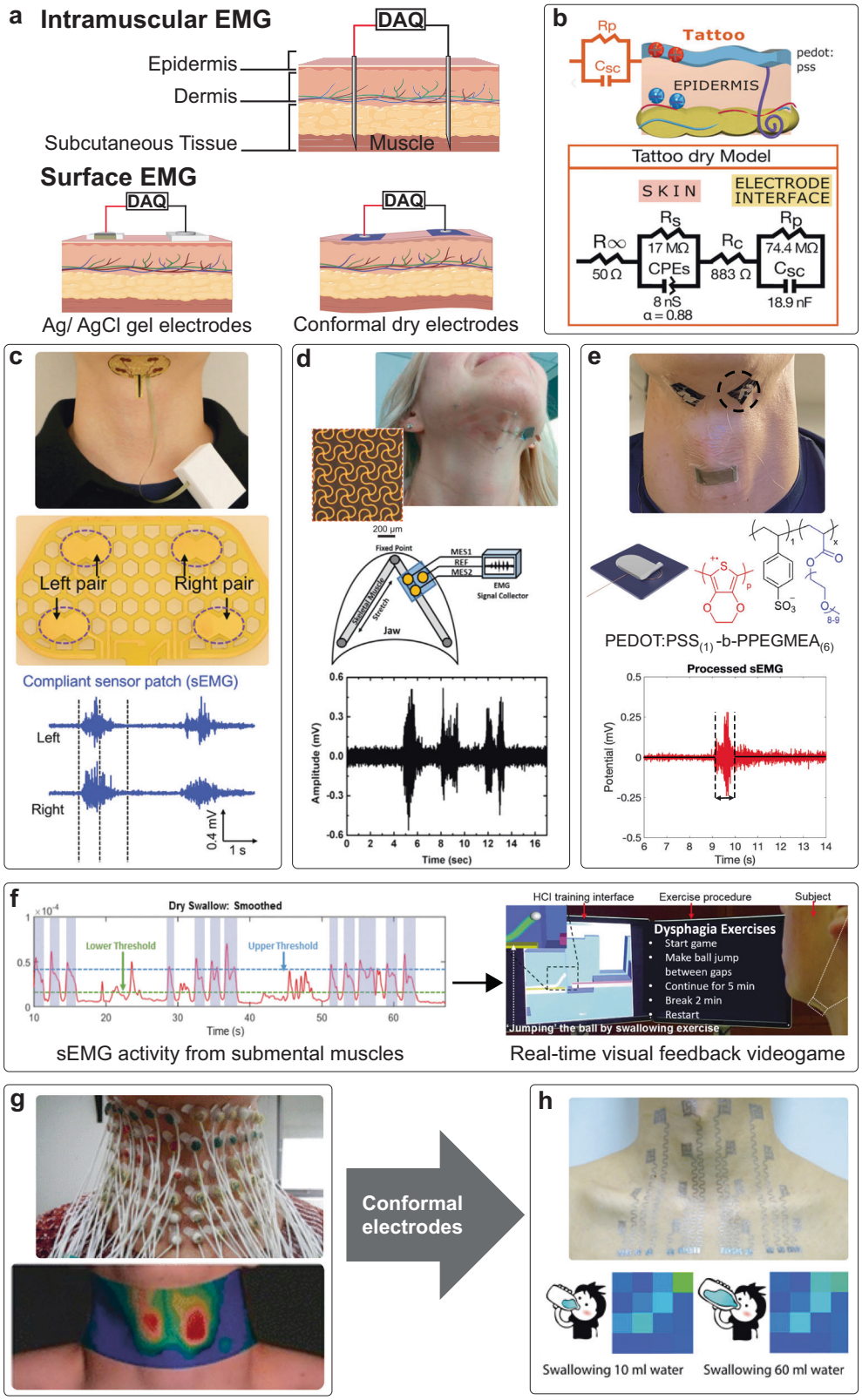

Fig. 2 Overview of conformal electromyography electrodes applied to swallowing tests. a A comparative schematic of EMG electrode types: Intramuscular (needle) EMG, gel sEMG electrodes, and conformal electrodes (in this case resembling dry polymer electrodes). **b** Equivalent circuit model of polymer-based (PEDOT:PSS) sEMG electrodes on the skin. **c**–**e** Epidermal conformal electrodes with their respective placements, sensor geometry, and sample outputs for the shown placement. **f** Shows the electromyographic data from submental muscles and the application of the electrodes in a swallowing exercise game. **g**, **h** Multichannel array of sEMG electrodes for swallowing mapping showing the contrast between the obstructive system based on classical electrodes in **g** and the thin epidermal patch in **h**. Both figure boxes demonstrate the output biopotential map during select stages of the swallow. Panels **b**, **d** reproduced with permission[88,92] Panels **c**, **e**–**h**, reproduced under Creative Commons (CC BY) license[53,105,109,112,121].

dioxythiophene):poly(styrene sulfonate) (PEDOT:PSS) have gained traction as an alternative bioelectronic material. The electrical conductivity of the polymer arises from the delocalization of electrons along the alternating single and double bonds, known as π-conjugation. Electrodes based on PEDOT:PSS show low interfacial impedances with skin owing to the high volumetric capacitance and mixed ionic and electronic conductivities in an interpenetrated, 3D network of conductive pathways. Although the intrinsic electrical conductivities are lower than metallic counterparts, many doping strategies have been exploited to provide additional paths for charge carriers along the polymer backbone by inducing favorable morphologies[113]. Moreover, it is possible to tune the elastic modulus to match the location on the skin and increase the durability of such polymers with additives and cross-linkers. Additives such as sorbitol, xylitol, Zonyl FS-300, Triton X-100, and ionic liquids are commonly used in the literature[114–118]. However, these additives have the potential to leech and are not always biocompatible.

Copolymerization is an attractive alternative method of plasticization without the need for molecular additives[119]. For example, the block copolymer of PEDOT:PSS with poly(poly(ethylene glycol) methyl ether acrylate) (PPEGMEA) augments the stretchability of the intrinsically brittle neat PEDOT:PSS[120]. By varying the blocks of $PEDOT:PSS_{(1)}$-*b*-$PPEGMEA_{(x)}$ from ($x \in \{1, 2, \ldots 6\}$), the elastic modulus can be reduced to ~10MPa, a magnitude lower than commercially available material. A recent study utilized $PEDOT:PSS_{(1)}$-*b*-$PPEGMEA_{(6)}$ electrodes placed on the submental region for swallow volume estimation during exercise. It was demonstrated that electrodes were effective for long-term capturing muscle activity despite the bodily motion (Fig. 2e)[121].

Measured impedances tend to decrease with time when suspended on the skin because of the presence of a sweat layer enriched with electrolytes. Based on the capacitive coupling (Fig. 2b), the resistance value, R_s, is extracted from sweat ducts found in the skin[88]. Therefore, the porous structure of PEDOT:PSS allows for the uptake of water, which can reduce the resistance values and perform as a breathable (vapor-permeable) wearable substrate[88,122]. The solution processability of this polymer makes for facile molding of freestanding sEMG in the desired geometric designs[121], and the adaptation of conformal and noise filtering geometries (see "Sensing mechanism and figures of merit"). Generally, liquid phase processability is an attractive material trait that allows facile and scalable fabrication of stretchable electronics. Such fabrication approaches include spin-casting, spray coating, dip coating, direct ink writing, and stamping, which can generate thin and conformal films on a variety of substrates[116,123–126]. In cases where the conductive material is being solvated, the concentration of the solution could be varied to modulate the electronic and mechanical properties of the film[127]. Collectively, the tunable characteristics, sensing abilities, biocompatibility, and processability are unique advantages of conducting polymers.

Ultrasensitive strain-gauge wearable sensors. The mechanical motion of subcutaneous anatomy exerts mechanical loads on the skin typically resulting in bending, stretching, compression, torsion, and wrinkling. This is typically exemplified in the dynamic skin tension in joint motion[128–130]. Stress generated by bending joints, expanding lungs, contracting muscles, and laryngeal motion among others strain the skin to various extents. Strain gauges placed on the throat and submental region translate the incurred bending or tensile strain, caused by swallow action, to an electrical signal (Fig. 3a). Studies implementing this modality have examined skin deformation due to muscle contractility in the submental/submandibular region or the motion of the larynx. The larynx moves by less than 1 cm anteriorly during a swallow generally causing protrusions in the skin[131]. These protrusions are most pronounced near the laryngeal prominence (LP) and cricoid cartilage. As the larynx traverses vertically, its motion can be measured using mechanical sensors (Fig. 1e *(right)*).

Strain gauges, among other wearable sensors, are inherently benign and non-invasive. Recent developments in organic and inorganic nanomaterials have led to many methods to render them more unobtrusive, stretchable, and skin-conforming. From applications in electronic skin to heart rate monitoring, strain gauges come in a range of signal outputs, sensitivities, compliances, and scales[8,132–135]. These mechanisms of strain gauges can be categorized into piezoresistive (geometrically induced effects), piezoelectric, capacitive, and optoelectronic[134]. Classical resistive strain gauges and flex sensors are often made from patterned rigid metal alloys carried by flexible polymer substrates. The rigidity of the constituent materials makes it difficult to apply conformally to the skin. Organic conductors, carbon-based nanomaterials (graphene, carbon nanotubes (CNT), etc.), and nanoscale particles (nano-spheres, nanowires, nanoislands, etc.) pose a class of stretchable piezoresistive strain gauges, with sensitivities high enough to detect muscle movements with extremely high sensitivities. Forming composites from conductive fillers and skin-compatible polymer hosts or substrates (PDMS, PU, Ecoflex, etc.), is the most common path to making piezoresistive strain gauges and is commonly adopted in literature. The figure of merit that is associated with piezoresistivity is the gauge factor (GF), as defined in Eq. 3 (see "Sensing mechanisms and figures of merit").

Carbon-based materials, such as graphene and CNTs are perhaps some of the most utilized in the literature on strain gauges[74,90,121,136–139]. In one example, Roh et al. reported a three-layer stacked strain sensor made up of single-wall carbon nanotubes (SWCNTs), PEDOT:PSS, and polyurethane (PU) (Fig. 3b)[139]. In lower strain regimes, the stretching of the elastomeric matrix increases the distance between conductive particles. As the strain increases, the conductive pathways break. The addition of PU-PEDOT:PSS conductive polymer ensures that during extreme stretching, some conductive pathways are retained, hence increasing the dynamic range. Previous work done by our group, utilizing single-layer graphene/gold nanoisland (Gr/AuNI) strain sensors, has shown that the addition of a plasticized PEDOT:PSS ("dough") layer (Fig. 3c) increased the stretchability of the piezoresistive film from more than 40 fold (2% to 86%)[90,121].

Systems of ultrahigh stretchability can also be made using hydrogels and organogels[130,138]. For instance, MXene, which is a class of inorganic conductors, nanosheet introduced to gluten networks showed strain ranges of up to 300% with a GF = 3.2[105]. The shape, color, and optical transparency of the resultant sensor are also important factors to consider when dealing with prolonged device use. Hwang et al. report low-density silver nanowires (AgNWs) with PEDOT:PSS/PU to fabricate a strain sensor[140]. This sensor showed high and uniform optical transparency (~75.3%), with stretchability (up to 100%), and sensitivity to strain (GF = 12 for 2% strain). Another example utilizing MXenes is a highly stretchable (~1200%) strain sensor made self-healable using polyvinyl alcohol (PVA) composite hydrogel matrix. This sensor incorporates a $Ti_3C_2T_x$ filler to form electrodes for a capacitive sensor. The sensor achieved a reasonable capacitive GF of (~0.4) and exceptional self-healability after 150 ms while retaining 97.5% capacitance after breakage. Proof-of-concept studies demonstrate the ability of this sensor to measure deformations (Fig. 3e) correlated with the four stages of a swallow (Fig. 1b)[141]. The strains caused by a laryngeal rise or muscle contractions are small compared to limb and finger joints, where such sensors are often applied. Hence, large dynamic ranges (e.g., >50%) are generally not required (Fig. 3f)[74]. Nevertheless, many of the sensor systems reviewed here have a sufficiently large strain range to capture the motions of the posterior neck, elbow, and knee joints, and face (Fig. 3g)[130,138,142,143].

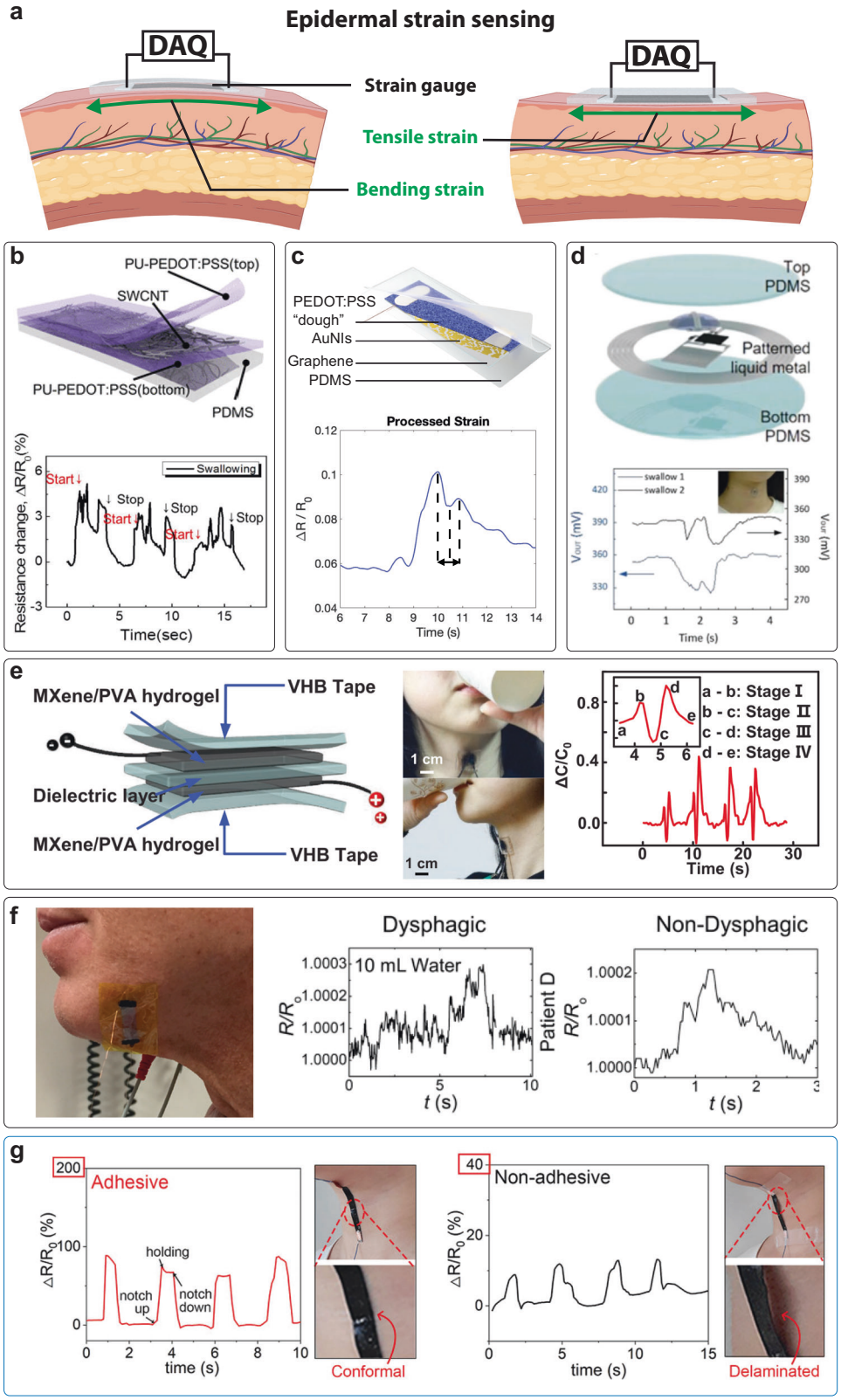

Fig. 3 Overview of materials-based wearable strain gauges applied in swallowing examination. a Epidermal strain sensors reacting to typical skin bending and tensile strains with the appropriate data acquisition systems connected to them. **b–d** Example strain-gauge schematics showing active materials and encapsulants with a sample swallow strain signal respectively. **e** PVA/ MXene-based capacitive sensor with sample signal expressing laryngeal motion in four stages. **f** Submental swallow activity monitoring using palladium nanoislands on graphene sensor, comparing dysphagic and non-dysphagic signal outcomes. **g** Comparative pictures, and corresponding plots demonstrating the effect of conformal adhesion on strain-gauge response. Panels **b**, **e**, **f**, **g**, reproduced with permission[74,139,141,143] Panels **c, d** reproduced under Creative Commons (CC BY) license[121,145].

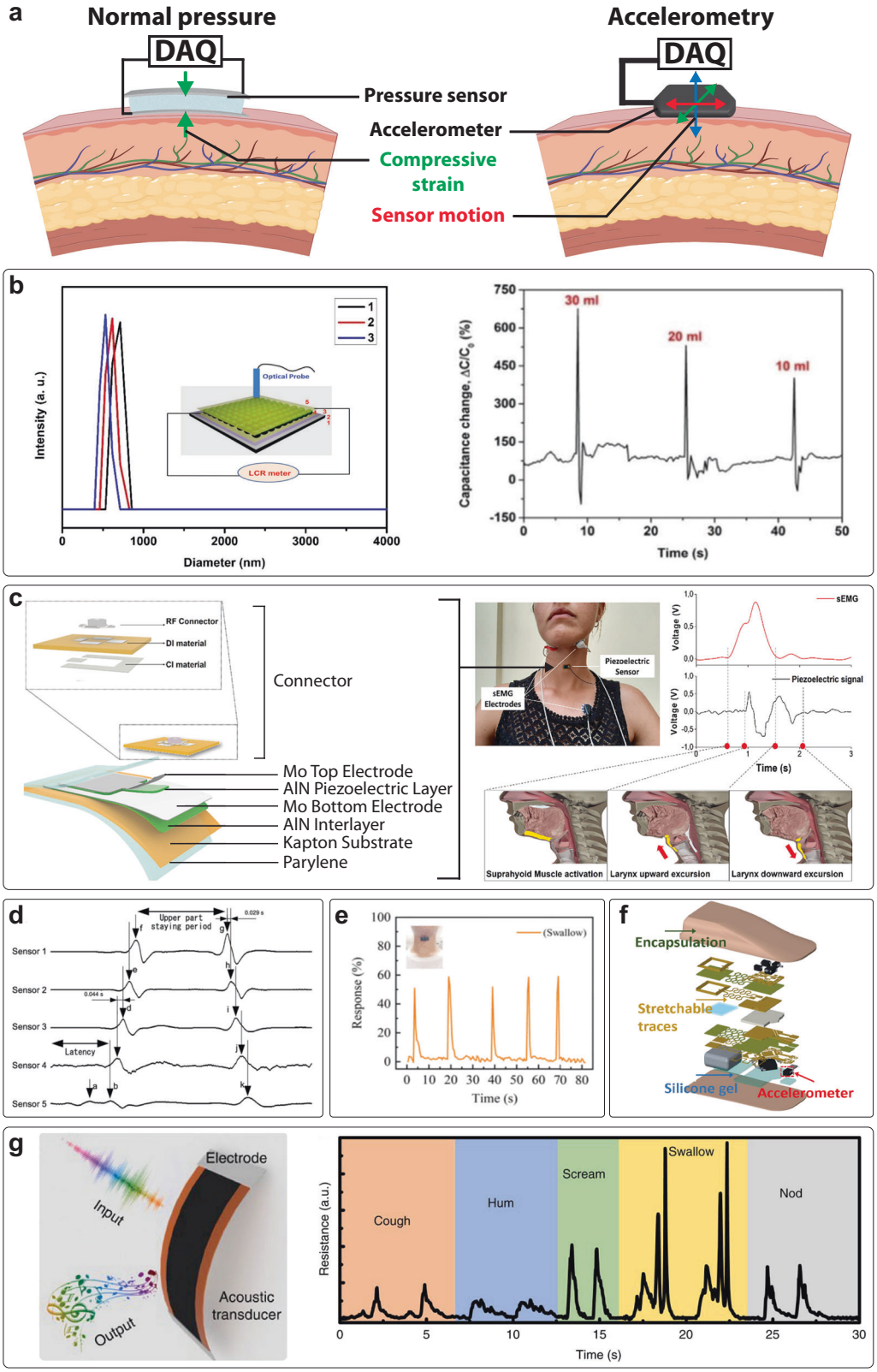

Liquid metal has also been used to generate patterned resistive sensors and circuits[144]. Jeong et al. utilized the wetting properties of reduced liquid metal alloy (GaInSn), to create a wireless patch for remote strain sensing with robust electrical and mechanical performance (Fig. 3d)[145]. The resistive strain-gauge component fabrication was enabled by exploiting the wetting phenomena of GaInSN on micro-patterned gold serpentines. A proof-of-concept demonstration showed the device detecting swallow activity and 10,000 cycles of reversible stretching.

Fig. 4 Overview of materials-based pressure sensors and accelerometric sensors applied in swallowing examination. a Typical epidermal pressure sensor reacting to compression caused by skin bending (left), and a mechano-acoustic/ accelerometric sensor reacting to skin motion and deformation. **b** Optical response from porosity diameter reduction (left) and capacitive response outputs in swallowing experiments demonstrate sensitivity to the consumed bolus volume (right). **c** A small profile piezoelectric swallowing pressure sensor based on AlN active material. Sensor outputs are shown to correspond with laryngeal motion and muscle activity signals. **d** Temporal parameters extracted from a piezoelectric array. **e** Reduction of resistance from pressure exerted during swallowing. **f** Mechano-acoustic sensor patch based on an IMU and a stretchable circuit geometry providing a non-obtrusive attachment and robust wireless data outputs. **g** Laser-induced graphene acoustic sensor, with distinctive signal outputs for various throat-related activities including swallowing. Panels **b**, **d**–**f** reproduced with permission[73,152,154,158] Panels **c**, **g** reproduced under Creative Commons (CC BY) license[155,163].

Pressure-based wearable sensors. Unlike strain sensing, pressure sensors generate a signal when compressed by a net force normal to the skin surface (Fig. 4a, left panel). This mode of operation allows these sensors to occupy generally smaller skin areas than strain or sEMG. The applications of wearable pressure sensors can be similar to those seen for strain sensors, but they see larger applications in artificial skins and wearable touch pads[146–150]. Reported swallow pressure sensors can be parsed into groups by their mechanism of transduction capacitive, optical, piezoelectric, or piezoresistive. The literature reports several permutations of materials for the electrodes and the dielectric media for capacitive sensors. Kou et al. described a wireless system developed around an NH_4HCO_3/Gr/PDMS dielectric sponge capacitor The sponge dielectric architecture, widely adopted in literature, imparts higher deformability onto the device (see "Signal acquisition and figures of merit" section) enhancing its lower detection limit (5 Pa) and lowering its response time[151]. The small planar form factor of the sensor allowed for a patch-mounted antenna for wireless and battery-free transmission. This was primarily enabled by the change in resonant frequency (f_{res}) of the inductor-capacitor (LC) circuit when the capacitance (C) varies due to compression ($f_{res} \propto LC^{-1/2}$). Although high in sensitivity elastomer foams tend to be on the order of 1 mm in thickness, which can make the device thicker and less skin-conforming. Thinner dielectric materials (~500 nm) have been examined for swallowing applications. Xia et al. applied a monolayer of colloidal microgel (free-radically polymerized N-isopropyl acrylamide (NIPAm), N, N'—methylene bisacrylamide, and acrylic acid (AAc)) that functioned as both a dielectric and an optical sensor ("etalon"), giving the sensor a dual response to pressure change[152]. By utilizing colloidal photonic crystals, swelling, and deswelling of the constituent microgel results in a spectrum of optical and capacitive sensitivity to pressure. In this work, ethanol was used to deswell the microgel resulting in a ~130 nm reduction of diameter and a change in optical signal (Fig. 4b, left panel). In principle, mechanical pressure exerted during swallowing could compress the microgel to generate a dual response. However, the optical response sensitivity, represented as a shift in the reflectance spectrum, was much lower than that seen in the capacitive aspect of this device. As a proof-of-concept, the change of capacitance was used to differentiate between water volumes (10–30 mL) with larger volumes corresponding to higher signal amplitudes (Fig. 4b, right panel). To that, a simpler optical approach can be generated using fiber optics. For instance, Maeda et al. used a hetero-core fiber optic pressure sensor embedded in a silicone rubber housing and measured the optical loss due pressure-induced deforemation[153].

Piezoelectric materials have seen many applications as wearable technologies in general (in ultrasonic and mechanical sensors) and in swallow evaluation in specific, despite their intrinsic rigidity. The use of common piezoelectric polymers such as polyvinylidene fluoride (PVDF) was demonstrated in a paper by Iizuka et al. where a urethane sheet was lined with piezoelectric sensors and placed near the LP[154]. The piezoelectric array captured the upper and lower laryngeal movement during swallowing in healthy subjects. Parameters such as swallowing latency and maximum lowering and rising velocities were characterized (Fig. 4d). By fixing the pitch at 3 mm, the velocity can be extracted by measuring the time difference between sensors' responses. Velocity responses of the laryngeal movement are complementary measurements to subjective evaluation (speech pathologist), as slow velocity is correlated to clinical aspiration. However, the total thickness of the array required the sensor to be placed by hand, which hindered decoupling bending motions along the axis of the laryngeal movement. To address such issues, researchers opt for thinner and unobstructive form factors. A recent example is the work by Natta et al. which featured patterned, ultra-thin, and flexible piezoelectric aluminum nitride (AlN) film mounted on a soft Kapton tape coupled with sticky PDMS-polyethyleneimine (PEIE) to make a sensor with a total thickness of 26 μm[155]. The sensitivity of this device can capture the pressure produced by the bolus passage (up to 50 KPa). Using this sensor, they were able to extract certain important factors from the data such as the duration of the swallowing act, frequency of spontaneous saliva deglutition, and latency (Fig. 4c). Specifically, the deglutition wave (upward and downward of the laryngeal movement) is measured from the voltage responses. Ideally, the deglutition wave consists of two peaks resembling the distinct phases of a swallow. The voltage peaks are responses when the laryngeal pushed the sensor during elevation and descent, respectively. Distortion of the deglutition waveform may infer swallowing abnormality. Also, delay in latency during deglutition is common in elderly patients with reduced motor units[156]. These temporal parameters provide complementary clinical insights into swallowing behavior, which can guide the assessment of swallowing abnormality. The authors also highlighted the superiority of AlN non-toxicity, biocompatibility, and superiority over PVDF piezoelectrics which degrade under heat exposure. Finally, wireless Bluetooth technology was utilized to transfer the collected sensor data into a phone application for a proof-of-concept of untethered point-of-care. Moreover, Lee et al. proposed a pressure sensor comprised of ionic polymer–metal composite (IPMC) material for recognizing throat movements during a swallow[157]. Essentially, a pressure applied to the IPMC induces cations and water molecules to move from high to low-stress regions and create a charge distribution while forming a dielectric potential layer. They also utilized a machine-learning algorithm, a support vector machine (SVM) model, to calculate the performance of throat movement detection of the sensor in different activities (e.g., coughing, swallowing, and humming). The double peak present in swallow signals increased the precision of the model (~96%) in differentiating it from other throat motions. Although more commonly used in the strain modality, piezoresistivity can also be used to sense pressure exerted by laryngeal motion. Guan et al. used a molybdenum diselenide/multi-walled carbon nanotubes ($MoSe_2$/MWNTs) composite capped with PDMS and copper foil electrodes on either side. Among the biosensing demonstrations in this work, the authors placed the sensor above the laryngeal prominence of a male subject and observed swallowing signals as a reduction in the resistance of the sensor (Fig. 4e)[158].

Acoustic and accelerometric devices. Many of the movements produced by swallowing produce acoustic signals and vibrations

that can be detected at the surface of the skin. Thus, wearable devices featuring MEMS accelerometers and acoustic sensors have the potential to advance traditional diagnostic methods based on auscultation (listening)[159,160]. Specifically, laryngeal microphones (laryngophones), have been applied to the assessment of dysphagia[161,162]. Unlike strain and pressure sensors which deform with muscular and laryngeal motions, vibration and audio signals encompass a larger range of deformation frequencies (from skin motion to audible swallow sounds)[64,161,162]. For instance, Tao et al. utilized a laser-induced graphene film that could generate and detect sounds from the skin[163]. This acoustic sensor used direct laser writing (450 nm wavelength) on polyimide (PI) substrates to raster porous graphene films[164]. This porous film structure allowed the detection of weak vibrations (such as vocal sounds) permeating the skin through its high degree of piezoresistance. When placed on the throat, this sensor was able to detect the swallowing activity among other physiological and bioacoustic signals (Fig. 4g). Examining the placement and signal amplitude of the device, however, indicates that the swallow signal reported is in part due to large-scale deformations of the sensor, and not just acoustic vibrations. Significant developments have been made in adapting commercial embedded circuits, such as MEMS-based inertial measurement units (IMUs), which can output gyroscopic and accelerometric data, into stretchable and skin adhesive platforms (Fig. 4f)[73]. Using buckled metal interconnects and elastomer substrates, IMUs, and microcontrollers can be mounted onto the skin to achieve close mechanical coupling. This coupling enables the system to detect acoustic vibrations (due to breathing, heart activity, and esophageal contraction). Differential measurements between two accelerometer devices were shown to reduce motion artifacts generated from routine day activities[64].

Multimodal sensors systems. Obtaining distinct data streams is a key factor in producing robust and efficient machine-learning algorithms and statistical models[165]. Multimodal sensors are relatively new in monitoring swallowing behavior. Early studies that have performed large-scale user testing with their sensors generally combine multiple modalities for cross-validation, a common combination is sEMG with strain or pressure measurement (e.g., Figs. 2e and 3c)[105,121,152]. Other studies use a single modality of sensing outputting several orthogonal data streams such as mechanical deformation along a different axis or the activation of various muscle groups[74,92,141]. Another added benefit of having multiple data streams is failure redundancy. In dysphagia assessment and treatment, for instance, the origin of the disorder can affect the applicability of certain modalities. sEMG swallow assessments show lower precision in diagnosing dysphagia arising from neurological disorders[166]. Additionally, comorbidities of dysphagia, either from shared etiology or completely unrelated ones, can reduce the efficacy of certain wearable modalities. For example, lymphedema in the neck area, commonly occurring after radiation cancer treatment, can cause the attenuation of biopotential signals and skin deformations in targeted areas[167]. Edema-induced attenuation effect has been observed with electrocardiogram (ECG) signals[168]. Radiation therapy can also injure the skin on the throat resulting in short-term desquamation and a reduction in necessary contact and adhesion[169]. Similarly, injuries and surgical scars can complicate the wearability of such epidermal devices. Further, extreme differences in morphologies associated with obesity or severe weight loss can greatly affect the reliability of the sensor (by signal attenuation or suboptimal placements)[168,170]. Addressing such challenges is critical since nutrition, hydration, and feeding disorders in general, apart from dysphagia, are of interest in swallowing sensors research[90,121,171,172]. Hence, having hybrid systems, containing an ensemble of sensors can help increase the fidelity of analysis, function as a contingency measure for patients with obstructive comorbidities, and increase the applicability to a wider range of users.

Sensing mechanisms and figures of merit

Since wearable swallow sensors are still developing, they are yet to stem well-established metrics for evaluating swallows specifically. Even though swallow health and some of its metrics (like speed, posture, and muscular effort) can be evaluated with wearable sensors, there are currently no overarching mathematical descriptions that can summarize the outcome. However, intertwined within each sensing modality discussed in this work, are the mechanisms that enable a sensor to detect and translate the input it receives to its respective signal. Each sensing mechanism can call for a unique data acquisition and analysis technique. Associated with these techniques are derived metrics and figures of merit some of which are discussed in this section.

EMG biopotential. The EMG signal arises from the depolarization of skeletal muscle fibers. When probed from the surface, the signals ought to contain the firing action of the collective of fibers under the electrodes. This contrasts with the fiber-targeting, yet invasive, approach in needle EMG[80]. The raw signal output amplitude of EMG is typically 0–10 mV_{pp} with the energy concentrated in the 20–500 Hz frequencies[173]. Knowing the frequency range of EMG allows for the implementation of filters, such as a 10–20 Hz high-pass filter for low-frequency noise and ECG signals and notch filters for powerline interference[174]. These measures serve to improve the signal-to-noise ratio (SNR); a common metric used to quantify signal quality defined as the ratio of signal power P_{signal} to noise power P_{noise}.

$$\mathrm{SNR} = \frac{P_{\mathrm{signal}}}{P_{\mathrm{noise}}} = \left(\frac{A_{\mathrm{signal}}}{A_{\mathrm{noise}}}\right)^2 ; \text{where } A \text{ is the amplitude} \quad (1)$$

The SNR of an sEMG system can give information about the electrode-skin contact and the effectiveness of the electrode placement. Poor electrode-skin contact, as mentioned earlier, can be a source of noise and unwanted motion artifacts, while an incorrect placement of the electrodes can generate interference potentials from unwanted muscular and neural activity[80]. Concentric electrode geometry has been shown to address some of these issues by localizing the target muscle and creating spatial (Laplacian) filtering effects. The Laplacian filter can be described by the following equation for a bipolar electrode:

$$L_{\mathrm{Bp}} = \frac{4}{(2_{r2})}(V_{\mathrm{o}} - V_{\mathrm{D}}) \quad (2)$$

where L would be the filtered biopotential signal, V_o and V_D are the potentials at the center and the circumference of radius r circle, respectively[175–177].

Piezoresistivity. When an external force deforms a piezoresistive material its electrical conductivity changes. Granted that this change is reversible, it can be used to continuously detect deformations. The correlation between strain and resistance can present itself in a linear or nonlinear fashion over the strain range of the material. Since linearity is typically favored for simpler data analysis, researchers favor the linear regimes of the material. Some patterned metal conductors can also be sensitive to strain despite having low intrinsic piezoresistivity. Geometric effects such as elongation or necking (cross-section constriction) imparted by applied stresses, change the overall resistance while maintaining the intrinsic conductivity. The figure of merit describing piezoresistive sensitivity is the gauge factor (GF): the normalized change in resistance $(\Delta R/R_o)$ with respect to changes in strain $(\varepsilon = \Delta\ell/\ell_o)$. Many devices reported in the literature contain two linear regimes owing to a variation in the conducive pathways. In this case, the sensor is given two GFs, one for each strain regime.

For initial resistance and length R_o and ℓ_o, respectively:

$$\mathrm{GF} = \frac{\Delta R/R_o}{\Delta \ell/\ell_o} \tag{3}$$

Resistive strain gauges are amenable to several data acquisition techniques apart from standard Ohmmeter measurements. Classically strain gauges can be probed with Wheatstone bridge circuits[178]. However, bridge circuit configurations can become complex especially when connecting multiple strain sensors to the circuit. Incorrect balancing of the bridge can also pose a challenge, especially for high-sensitivity sensors, ones with varying baseline resistances, and those with a significant temperature coefficient of resistance (TCR). The alternatives include using a constant current into the leads of the sensor and probing the voltage drop occurring across it or using digital multimeters[179].

Capacitive sensitivity. Typically, a capacitor is a charge-storing device that can be visualized as two electrodes separated by a dielectric medium. The amount of charge that it can theoretically store is dependent on the permittivity of the materials (ε), the area of the electrodes (A), and the electrode separation (d). A mechanical input into a capacitive sensor can change these variables causing a measurable change in capacitance. In the parallel plate configuration, the dielectric material is usually composed of soft elastomer that compresses to change the electrode proximity. Often, the polymer dielectric is made porous or patterned with microstructure to impart a range of compliance and reduce the viscoelastic effects[132,146,180]. These measures can work to reduce the latency of the sensor and its hysteresis by virtue of optimizing the viscoelastic properties[146]. Other designs, such as interdigitated capacitive sensors, while they produce the same effect do not necessarily change their inter-electrode distance. They instead rely on variability in the dielectric material structure for a change in the dielectric constant[181].

$$C = \frac{\varepsilon A}{d} \tag{4}$$

$$I = C\frac{dV}{dt}; \text{where } I \text{ is current and } t \text{ is time} \tag{5}$$

Like the gauge factor of piezoresistive materials, some literature sources define a GF for capacitive sensors where the numerator denotes $\Delta C/C_o$. However, capacitive sensors are popular in the pressure modality; hence they undergo compressive forces. In cases where compressive strain is difficult to quantify due to internal geometric complexity or scale, the sensitivity could be defined in terms of stress (pressure):

$$S_{\text{capacitive}} = \frac{\Delta C/C_o}{\Delta P} = \frac{\Delta C/C_o}{\Delta F/A} \tag{6}$$

where ΔC is the change in capacitance due to loading pressure ΔP. The sensitivity figure S can be defined for any sensing mechanism where there is a defined baseline signal (in this case C_o) and change the signal change commensurate with the input pressure. If the area on which the force is exerted is assumed to be constant, the pressure change can be broken down in Eq. 6. Capturing the capacitance signal tends to be a more challenging task when compared with resistance. Most of the proof-of-concept sensor papers utilize tethered and stationary LCR (inductance, capacitance, resistance) meters or customized acquisition systems[151,152,181,182]. However, as mentioned earlier these sensors can be integrated into wireless, battery-free devices utilizing antennas to create an LC (inductor-capacitor) circuit whose resonant frequency is a function of capacitance.

Piezoelectricity. Piezoelectric materials have seen many transducer applications in wearable technologies, both as actuators and sensors. Their ability to intrinsically generate voltage signals from mechanical input omits the need for powering the sensor[183]. However, depending on the active materials and their size, the output signals will often require significant amplification. The lattice structure of a piezoelectric material determines its response to different mechanical inputs. Like the sensitivity defined for capacitive sensors, sensitivity can be defined for piezoelectric sensors:

$$S_{\text{piezoelectric}} = \frac{\Delta V}{\Delta P} \tag{7}$$

The described mechanisms are those associated with flexible and stretchable sensors. These figures of merit can be used to compare different sensors. In research settings, various data acquisition systems are used to probe signal outputs as mentioned earlier. Recent developments of low energy and compact data acquisition systems have allowed for the dispatching of these mechanisms into wireless platforms[155,184]. Apart from signal clarity, the latency of the signal is also an important factor. The time delay associated with signal transduction can vary with the signal acquisition system, as well as the mechanical response of the sensor material. More mature wearable sensing mechanisms such as accelerometry and audio signal recordings offer robust signal outputs that can be read with and have extensive support from development microcontroller boards (Arduino, Raspberry Pi, STMicroelectronics, etc.), or custom microcontroller boards.

Translation to the clinic and home use

The ultimate goal of the research in the area of wearable biomedical devices is to transition from the clinic to the home. Barriers to adoption are not, of course, limited to devices to assess swallowing function. However, if strategies for increased engagement and usability could be developed in this context, they could be applied to most types of epidermal devices. The ultimate success of such work would leverage nearly two decades of work on devices in flexible and stretchable form factors. To this end, we highlight two areas for continued research: user engagement and compliance, along with wireless telemetry and power.

User engagement and compliance. Engagement with devices is a challenge faced even by commercial technologies. Despite robust sales, 50% of fitness trackers are abandoned after 6-12 months of use. For older adults, engagement is worse: 43% of adults 70 and older reported abandoning devices within the first two weeks[185,186]. Methods to improve engagement possibly include using haptic or visual feedback to relay information on the health of the swallow or indicate its successful or unsuccessful execution[64,111,162]. A real-time feedback mechanism could also be coupled with swallowing exercise maneuvers, often prescribed to dysphagic patients, to portray success/failure metrics and maintain exercise pace. The stimulation of nerves to elicit tactile sensations by mechanical or electrical cues has been utilized in diverse biomedical applications such as prosthetics[187,188], robotic teleoperations[189], and biomedical assistive technologies[190,191]. Conventional mechanisms such as those found in handheld devices like eccentric rotating mass motors (ERMs) and magnetic linear resonant actuators (LRAs) are common in wearable technologies[192]. However, their rigid form factors can limit their integration in soft, dynamic, and curvilinear regions of the human body such as the neck[193]. Alternatively, devices for electrotactile stimulation can be implemented in a flexible or stretchable form factor[194,195]. These sensations can vary from sustained pressure, prickle, vibration, and itch[196]. In general, electrotactile devices require low power consumption when compared to mechanical actuators[197], but may suffer from issues such as desensitization of the skin or even pain[157]. Visual feedback of data in real-time (e.g.,

as a smartphone app) has also been explored as a means of increasing patient engagement, compliance, and adherence, but little such long-term results have been reported for swallowing devices[198].

Wireless telemetry and power. Prototypes of wearable devices developed in the laboratory are often tethered to non-portable equipment for analysis of the data. To enable continuous long-term monitoring of dysphagia in a home environment, system-level integration of various electrical components in a miniaturized patch is required[199]. Nevertheless, data processing is not expected to be performed on the wearable itself. Instead, the patch should communicate wirelessly with a personal device (i.e., phone or computer). Many wearable devices have integrated miniaturized electrical components, along with Bluetooth or near-field communication chips, in a stretchable encapsulant[200,201]. For efficient telemetry, it's common for the dimensions of the antenna to be at least one-quarter of the signal wavelength[202]. Other innovative modules demonstrate battery-free wireless power and data telemetry at large power densities for further miniaturization with magnetoelectric phenomena[203]. Parametric designs of the magnetoelectric substrate are paramount, as the resonant frequency and output voltage are a function of the thickness[204].

OUTLOOK AND CONCLUSION

The development of engaging yet physically unobtrusive epidermal devices has the potential to assist in the detection and treatment of swallowing dysfunction. The convenience and physical wearability of swallowing sensors have been greatly improved by the realization of flexible and stretchable electronic materials, such as elastomer composites, ionic hydrogels, conductive polymers, and patterned metal conductors. Research for such materials and their application to swallowing behavior is creating new modalities for the detection of swallow health (e.g., strain, pressure) and improving well-documented and previously researched ones (e.g., EMG and acoustic signals). Although the sensing mechanisms associated with such transducers are now established, challenges remain from data interpretation and communication to maintaining user engagement beyond single uses and healthcare provider buy-in. While data acquisition and communication may be improved using existing dispatchable controllers, and wireless communication platforms, the rest of the challenges require further investigation. Swallowing and feeding disorders such as dysphagia require long-term monitoring and care, a feat wearable swallowing sensors are yet to demonstrate in human studies, despite the promising robustness of the used materials. To that end, improvements in this area would entail longer-term examinations of durability and efficacy, and large sample size human subject trials. Another vital step to achieving continuous, passive, and mobile data collection, is the evaluation of sensors under non-stationary subject conditions and out-of-lab settings. These investigations can help identify undesirable artifacts coming from the user's body movement to identify appropriate data filters. In tandem, they would shed light on user adherence and engagement during swallowing therapies, a crucial facet in preventing swallowing and feeding disorders. Feedback systems (visual, auditory, and haptic), as discussed, can thereafter be effectively implemented to improve adherence and engagement metrics.

DATA AVAILABILITY

All the data are available within the article or available from the authors upon reasonable request.

Received: 21 June 2023; Accepted: 28 November 2023;
Published online: 20 December 2023

REFERENCES

1. Jones, B. *Normal and Abnormal Swallowing: Imaging in Diagnosis and Therapy*. (Springer, 2003).
2. Matsuo, K. & Palmer, J. B. Anatomy and physiology of feeding and swallowing: normal and abnormal. *Phys. Med. Rehabil. Clin. North Am.* **19**, 691–707 (2008).
3. Hiiemae, K. M. & Palmer, J. B. Food transport and bolus formation during complete feeding sequences on foods of different initial consistency. *Dysphagia* **14**, 31–42 (1999).
4. Eisbruch, A. et al. Dysphagia and aspiration after chemoradiotherapy for head-and-neck cancer: which anatomic structures are affected and can they be spared by IMRT? *Int. J. Radiat. Oncol. Biol. Phys.* **60**, 1425–1439 (2004).
5. Roden, D. F. & Altman, K. W. Causes of dysphagia among different age groups: a systematic review of the literature. *Otolaryngol. Clin. North. Am.* **46**, 965–987 (2013).
6. Hutcheson, K. A. et al. Late dysphagia after radiotherapy-based treatment of head and neck cancer. *Cancer* **118**, 5793–5799 (2012).
7. Garon, B. R., Sierzant, T. & Ormiston, C. Silent aspiration. *J. Neurosci. Nurs.* **41**, 178–185 (2009).
8. Argov, Z. & de Visser, M. Dysphagia in adult myopathies. *Neuromuscul. Disord.* **31**, 5–20 (2021).
9. Smithard, D. G. Dysphagia: a geriatric giant? The normal swallow. *iMedPub J.* **2**, 1–7 (2016).
10. Leslie, P., Carding, P. N. & Wilson, J. A. Investigation and management of chronic dysphagia. *Br. Med. J.* **326**, 433–436 (2003).
11. Humbert, I. A. & Robbins, J. A. Dysphagia in the elderly. *Phys. Med. Rehabil. Clin. North Am.* **19**, 853–866 (2008).
12. Fujishima, I. et al. Sarcopenia and dysphagia: position paper by four professional organizations. *Geriatr. Gerontol. Int.* **19**, 91–97 (2019).
13. Rofes, L. et al. Pathophysiology of oropharyngeal dysphagia in the frail elderly. *Neurogastroenterol. Motility* **22**. https://doi.org/10.1111/j.1365-2982.2010.01521.x (2010).
14. Shaik, M. R., Shaik, N. A., & Mikdashi J. Autoimmune dysphagia related to rheumatologic disorders: a focused review on diagnosis and treatment. *Cureus*. https://doi.org/10.7759/cureus.41883 (2023).
15. Stathopoulos, P. & Dalakas, M. C. Autoimmune neurogenic dysphagia. *Dysphagia* **37**, 473–487 (2022).
16. Rajati, F., Ahmadi, N., Naghibzadeh, Z. A.-s. & Kazeminia, M. The global prevalence of oropharyngeal dysphagia in different populations: a systematic review and meta-analysis. *J. Transl. Med.* **20**. https://doi.org/10.1186/s12967-022-03380-0 (2022).
17. Adkins, C. et al. Prevalence and characteristics of dysphagia based on a population-based survey. *Clin. Gastroenterol. Hepatol.* **18**, 1970–1979 (2020).
18. Serrano Cardona, L. & Muñoz Mata, E. Prevalence and risk factors for dysphagia: a U.S. community study. *Early Hum. Dev.* **83**, 1–11 (2013).
19. Park, Y. H. et al. Prevalence and associated factors of dysphagia in nursing home residents. *Geriatr. Nurs. (Minneap)* **34**, 212–217 (2013).
20. Clavé, P. & Shaker, R. Dysphagia: current reality and scope of the problem. *Nat. Rev. Gastroenterol. Hepatol.* **12**, 259–270 (2015).
21. Cooper, J. S., Fu, K., Marks, J. & Silverman, S. Late effects of radiation therapy in the head and neck region. *Int. J. Radiat. Oncol. Biol. Phys.* **31**, 1141–1164 (1995).
22. Nguyen, N. P. et al. Dysphagia following chemoradiation for locally advanced head and neck cancer. *Ann. Oncol.***15**, 383–388 (2004).
23. Hutcheson, K. A. et al. Eat and exercise during radiotherapy or chemoradiotherapy for pharyngeal cancers: Use it or lose it. *JAMA Otolaryngol. Head Neck Surg.* **139**, 1127–1134 (2013).
24. Roe, J. W. G., Drinnan, M. J., Carding, P. N., Harrington, K. J. & Nutting, C. M. Patient-reported outcomes following parotid-sparing intensity-modulated radiotherapy for head and neck cancer. How important is dysphagia? *Oral Oncol.* **50**, 1182–1187 (2014).
25. Feng, F. Y. et al. Intensity-modulated chemoradiotherapy aiming to reduce dysphagia in patients with oropharyngeal cancer: Clinical and functional results. *J. Clin. Oncol.* **28**, 2732–2738 (2010).
26. King, S. N., Dunlap, N. E., Tennant, P. A. & Pitts, T. Pathophysiology of radiation-induced dysphagia in head and neck cancer. *Dysphagia* **31**, 339–351 (2016).
27. Burkhead, L. M., Sapienza, C. M. & Rosenbek, J. C. Strength-training exercise in dysphagia rehabilitation: principles, procedures, and directions for future research. *Dysphagia* **22**, 251–265 (2007).
28. Strength, L. C. Tounge and exercise in healthy individuals and in head and neck cancer patients. *Semin. Speech Lang.* **27**, 260–267 (2006).

29. Carnaby-Mann, G., Crary, M. A., Schmalfuss, I. & Amdur, R. 'Pharyngocise': randomized controlled trial of preventative exercises to maintain muscle structure and swallowing function during head-and-neck chemoradiotherapy. *Int. J. Radiat. Oncol. Biol. Phy.s* **83**, 210–219 (2012).
30. Scheerens, C., Tack, J., & Rommel, N. Buspirone, a new drug for the management of patients with ineffective esophageal motility?. *United Eur. Gastroenterol. J.* **3**, 261–265 (2015).
31. Cheng, I., Sasegbon, A., & Hamdy S. Effects of pharmacological agents for neurogenic oropharyngeal dysphagia: a systematic review and meta-analysis. *Neurogastroenterol. Motility* **34**. https://doi.org/10.1111/nmo.14220 (2022).
32. Nakato, R. et al. Diagnosis and treatments for oropharyngeal dysphagia: effects of capsaicin evaluated by newly developed ultrasonographic method. *J. Smooth Muscle Res.* **56**, 46–57 (2020).
33. Martin-Harris, B. et al. Respiratory-swallow training in patients with head and neck cancer. *Arch. Phys. Med. Rehabil.* **96**, 885–893 (2015).
34. Ciarambino, T., Sansone, G., Para, O. & Giordano, M. Dysphagia: what we know? a minireview. *J. Gerontol. Geriat.* **69**, 188–194 (2021).
35. Høxbroe Michaelsen, S., Grønhøj, C., Høxbroe Michaelsen, J., Friborg, J. & von Buchwald, C. Quality of life in survivors of oropharyngeal cancer: a systematic review and meta-analysis of 1366 patients. *Eur. J. Cancer* **78**, 91–102 (2017).
36. Nguyen, N. P. et al. Aspiration rate following chemoradiation for head and neck cancer: an underreported occurrence. *Radiother. Oncol.* **80**, 302–306 (2006).
37. Eisbruch, A. et al. Objective assessment of swallowing dysfunction and aspiration after radiation concurrent with chemotherapy for head-and-neck cancer. *Int. J. Radiat. Oncol. Biol. Phys.* **53**, 23–28 (2002).
38. Palmer, J. B., Kuhlemeir, K. V., Tippett, D. C. & Lynch, C. A protocol for the videofluorographic swallowing study. *Dysphagia* **8**, 209–214 (1993).
39. Logemann, J. A. Role of the modified barium swallow in management of patients with dysphagia. *Otolaryngol. Head Neck Surg.* **116**, 335–338 (1997).
40. Martin-Harris, B., Logemann, J. A., McMahon, S., Schleicher, M. & Sandidge, J. Clinical utility of the modified barium swallow. *Dysphagia* **15**, 136–141 (2000).
41. Langmore, S. E., Kenneth, S. M. A. & Olsen, N. Fiberoptic endoscopic examination of swallowing safety: a new procedure. *Dysphagia* **2**, 216–219 (1988).
42. Badenduck, L. A. et al. Fiber-optic endoscopic evaluation of swallowing to assess swallowing outcomes as a function of head position in a normal population. *J. Otolaryngol. Head Neck Surg.* **43**, 2–7 (2014).
43. Bastian, R. W. Videoendoscopic evaluation of patients with dysphagia: an adjunct to the modified barium swallow. *Otolaryngol. Head Neck Surg.* **104**, 339–350 (1991).
44. Knigge, M. A., Thibeault, S., & Mcculloch T. M. Implementation of high-resolution manometry in the clinical practice of speech language pathology. *Dysphagia* **29**, 2–16 (2014).
45. Ryu, J. S., Park, D. & Kang, J. Y. Application and interpretation of high-resolution manometry for pharyngeal dysphagia. *J. Neurogastroenterol. Motil.* **21**, 283–287 (2015).
46. Antonios, N. et al. Analysis of a physician tool for evaluating dysphagia on an inpatient stroke unit: the modified Mann assessment of swallowing ability. *J. Stroke Cerebrovasc. Dis.* **19**, 49–57 (2010).
47. Somasundaram, S. et al. Dysphagia risk assessment in acute left-hemispheric middle cerebral artery stroke. *Cerebrovasc. Dis.* **37**, 217–222 (2014).
48. Warnecke, T. et al. Aspiration and dysphagia screening in acute stroke–the Gugging Swallowing Screen revisited. *Eur. J. Neurol.* **24**, 594–601 (2017).
49. Chen, P., Chuang, C., Leong, C., Guo, S. & Hsin, Y. Systematic review and meta-analysis of the diagnostic accuracy of the water swallow test for screening aspiration in stroke patients. *J. Adv. Nurs.* **72**, 2575–2586 (2016).
50. Wagner, S. & Bauer, S. Materials for stretchable electronics. *MRS Bull.* **37**, 207–213 (2012).
51. Kim, D.-H. et al. Epidermal electronics. *Science (1979)* **333**, 838–843 (2011).
52. Kaltenbrunner, M. et al. An ultra-lightweight design for imperceptible plastic electronics. *Nature* **499**, 458–463 (2013).
53. Wang, Y. et al. Electrically compensated, tattoo-like electrodes for epidermal electrophysiology at scale. *Sci. Adv.* **6**. https://doi.org/10.1126/sciadv.abd0996 (2020).
54. Shaw, S. M. & Martino, R. The normal swallow: muscular and neurophysiological control. *Otolaryngol. Clin. North Am.* **46**, 937–956 (2013).
55. Ertekin, C. & Aydogdu, I. Neurophysiology of swallowing. *Clin. Neurophysiol.* **114**, 2226–2244 (2003).
56. Logemann, J. A. *Evaluation and Treatment of Swallowing Disorders*. 2nd edn. (PRO-ED, Austin, 1998).
57. Dodds, W. J., Stewart, E. T. & Logemann, J. A. Physiology and radiology of the normal oral and pharyngeal phases of swallowing. *Am. J. Roentgenol.* **154**, 953–963 (1989).
58. Palmer, J. B., Rudin, N. J., Lara, G. & Crompton, A. W. Coordination of mastication and swallowing. *Dysphagia* **7**, 187–200 (1992).
59. Dua, K. S., Ren, J., Bardan, E., Xie, P. & Shaker, R. Coordination of deglutitive glottal function and pharyngeal bolus transit during normal eating. *Gastroenterology* **112**, 73–83 (1997).
60. Palmer, J. B. & Crompton A. W. Coordination of mastication and swallowing. **200**, 187–200 (1992).
61. Matsuo, K., Hiiemae, K. M. & Palmer, J. B. Cyclic motion of the soft palate in feeding. *J. Dent. Res.* **84**, 39–42 (2005).
62. Buettner, A., Beer, A., Hannig, C. & Settles, M. Observation of the swallowing process by application of videofluoroscopy and real-time magnetic resonance imaging-consequences for retronasal aroma stimulation. *Chem. Senses* **26**, 1211–1219 (2001).
63. Palmer, J. B. & Hiiemae, K. M. Eating and breathing: interactions between respiration and feeding on solid food. *Dysphagia* **18**, 169–178 (2003).
64. Kang, Y. J. et al. Soft skin-interfaced mechano-acoustic sensors for real-time monitoring and patient feedback on respiratory and swallowing biomechanics. *NPJ Digit. Med.* **5**, https://doi.org/10.1038/s41746-022-00691-w (2022).
65. Shaker, R., Dodds, W. J., Dantas, R. O., Hogan, W. J. & Arndorfer, R. C. Coordination of deglutitive glottic closure with oropharyngeal swallowing. *Gastroenterology* **98**, 1478–1484 (1990).
66. Ohmae, Y., Logemann, J. A., Kaiser, P., Hanson, D. G. & Kahrilas, P. J. Timing of glottic closure during normal swallow. *Head Neck* **17**, 394–402 (1995).
67. Logemann, J. A. et al. Closure mechanisms of laryngeal vestibule during swallow. *Am. J. Physiol.-Gastrointestinal. Liver Physiol.* **262**, G338–G344 (1992).
68. Cook, I. J. et al. Opening mechanisms of the human upper esophageal sphincter. *Am. J. Physiol.-Gastrointestinal Liver Physiol.* **257**, G748–G759 (1989).
69. Ertekin, C. & Aydogdu, I. Electromyography of human cricopharyngeal muscle of the upper esophageal sphincter. *Muscle Nerve* **26**, 729–739 (2002).
70. Daniels, S. K. & Easterling, C. S. Continued relevance of videofluoroscopy in the evaluation of oropharyngeal. *Dysphagia Curr. Radiol. Rep.* **5**, 1–9 (2017).
71. Lo Re, G. et al. Swallowing evaluation with videofluoroscopy in the paediatric population. *Acta Otorhinolaryngol. Italica* **39**, 279–288 (2019).
72. Bonilha, H. S., Huda, W., Wilmskoetter, J., Martin-Harris, B. & Tipnis, S. V. Radiation risks to adult patients undergoing modified barium swallow studies. *Dysphagia* **34**, 922–929 (2019).
73. Lee, K. et al. Mechano-acoustic sensing of physiological processes and body motions via a soft wireless device placed at the suprasternal notch. *Nat. Biomed. Eng.* **4**. https://doi.org/10.1038/s41551-019-0480-6 (2020).
74. Ramírez, J. et al. Metallic nanoislands on graphene for monitoring swallowing activity in head and neck cancer patients. *ACS Nano* **12**, 5913–5922 (2018).
75. Kantarcigil, C. et al. Validation of a novel wearable electromyography patch for monitoring submental muscle activity during swallowing: a randomized crossover trial. *J. Speech Lang. Hear. Res.* **63**, 3293–3310 (2020).
76. Steele, C. Treating dysphagia with sEMG Biofeedback. *ASHA Leader* **9**, 2–23 (2004).
77. Crary, M. A., Carnaby, G. D., Groher, M. E. & Helseth, E. Functional benefits of dysphagia therapy using adjunctive sEMG biofeedback. *Dysphagia* **19**, 160–164 (2004).
78. Ertekin, C. Electrophysiological evaluation of oropharyngeal dysphagia in Parkinson's disease. *J. Mov. Disord.* **7**, 31–56 (2014).
79. Wheeler, K. M., Chiara, T. & Sapienza C. M. Surface electromyographic activity of the submental muscles during swallow and expiratory pressure threshold training tasks. *Dysphagia* **116**, 108–116 (2007).
80. Reaz, M. B. I. & Hussain M. S. Techniques of EMG signal analysis: detection, processing, classification and applications. *Biol. Proced. Online* **8**, 11–35 (2006).
81. Vescio, B., Quattrone, A., Nisticò, R., Crasà, M. & Quattrone, A. Wearable devices for assessment of tremor. *Front. Neurol.* **12**, 1–7 (2021).
82. Iqbal, S. M. A., Mahgoub, I., Du, E., Leavitt, M. A. & Asghar, W. Advances in healthcare wearable devices. *npj Flex. Electron.* **5**, 1–14 (2021).
83. Sethi, A., Ting, J., Allen, M., Clark, W. & Weber, D. Advances in motion and electromyography based wearable technology for upper extremity function rehabilitation: a review. *J. Hand Ther.* **33**, 180–187 (2020).
84. Tao, W., Liu, T., Zheng, R. & Feng, H. Gait analysis using wearable sensors. *Sensors* **12**, 2255–2283 (2012).
85. Yamaguchi, T. et al. Portable and wearable electromyographic devices for the assessment of sleep bruxism and awake bruxism: a literature review. *Cranio J. Craniomandib. Pract.* **00**, 1–9 (2020).
86. Hary, D., Bekey, G. A. & Antonelli, D. J. Circuit models and simulation analysis of electromyographic signal sources—I: the impedance of EMG electrodes. *IEEE Trans. Biomed. Eng.* **34**, 758 (1987).
87. Grimnes, S. & Martinsen, Ø. G. Cole electrical impedance model-a critique and an alternative. *IEEE Trans. Biomed. Eng.* **52**, 132–135 (2005).
88. Ferrari, L. M., et al. Capacitive coupling of conducting polymer tattoo electrodes with the skin. *Adv. Mater. Interface* **2100352**, 1–8 (2021).

89. Ruzgas T. et al. Skin membrane electrical impedance properties under the influence of a varying water gradient. **104**. https://doi.org/10.1016/j.bpj.2013.05.008 (2013).
90. Polat, B. et al. Epidermal graphene sensors and machine learning for estimating swallowed volume. *ACS Appl Nano Mater* **4**, 8126–8134 (2021).
91. Dr. Vladimir, V. F. Hyoid movement and sEMG activity during normal discrete swallows, Mendelsohn maneuver, effortful swallow and expiratory pressure threshold tasks in healthy adults. *Gastronomía Ecuatoriana y Turismo local* **1**, 5–24 (1967).
92. Constantinescu, G. et al. Epidermal electronics for electromyography: an application to swallowing therapy. *Med. Eng. Phys.* **38**, 807–812 (2016).
93. Kendall, K. A. & Leonard R. J. Hyoid movement during swallowing in older patients with dysphagia. http://rsb.info.nih.gov/nih-image (2001).
94. Reimers-Neils, L., Logemann, J. & Larson, C. Viscosity effects on EMG activity in normal swallow. *Dysphagia* **9**, 101–106 (1994).
95. Ko, J. Y., Kim, H., Jang, J., Lee, J. C. & Ryu, J. S. Electromyographic activation patterns during swallowing in older adults. *Sci. Rep.* **11**, 1–10 (2021).
96. Zhang, K. et al. Tough hydrogel bioadhesives for sutureless wound sealing, hemostasis and biointerfaces. https://doi.org/10.1002/adfm.202111465 (2022).
97. Yang, C. & Suo, Z. Hydrogel ionotronics. *Nat. Rev. Mater.* **3**, 125–142 (2018).
98. Wang, C. et al. On-skin paintable biogel for long-term high-fidelity electroencephalogram recording. *Sci. Adv.* **8**, 1–12 (2022).
99. Lee, H., Kim, C. & Sun, J. Stretchable ionics—a promising candidate for upcoming wearable devices. **1704403**, 1–15 (2018).
100. Yuk, H., Lu, B. & Zhao, X. Hydrogel bioelectronics. *Chem. Soc. Rev.* **48**, 1642–1667 (2019).
101. Bai, Y. et al. Transparent hydrogel with enhanced water retention capacity by introducing highly hydratable salt. *Appl. Phys. Lett.* **151903**. https://doi.org/10.1063/1.4898189 (2019).
102. Robinson, R. A. Ionic hydration and activity in electrolyte solutions. *J. Am. Chem. Soc.* **70,** 1870–1878 (1948).
103. Dang. W., Vinciguerra V., Lorenzelli L. & Dahiya R. Printable stretchable interconnects. *Flex. Print. Electron.* **2**, 013003 (2017).
104. Rafeedi, T. & Lipomi, D. J. Multiple pathways to stretchable electronics. *Science* **378**, 6625 (2022).
105. Kim, M. K. et al. Flexible submental sensor patch with remote monitoring controls for management of oropharyngeal swallowing disorders. *Sci. Adv.* **5**, 1–10 (2019).
106. Yang, S. et al. 'Cut-and-Paste' manufacture of multiparametric epidermal sensor systems. *Adv. Mater.* **27**, 6423–6430 (2015).
107. Malvuccio, C. & Kamavuako, E. N. Detection of swallowing events and fluid intake volume estimation from surface electromyography signals. *Proceedings-2020 IEEE EMBS Conference on Biomedical Engineering and Sciences, IECBES 2020*. 245–250 (IEEE, 2021).
108. Koyama Y., Ohmori N., Momose H., Yamada S. I. & Kurita H. Detection of swallowing disorders with a multiple-channel surface electromyography sensor sheet. *J. Dent. Sci.* https://doi.org/10.1016/j.jds.2021.12.015 (2022).
109. Zhu, M. et al. Evaluation of normal swallowing functions by using dynamic high-density surface electromyography maps. *Biomed. Eng. Online* **16**, 1–18 (2017).
110. Norton, J. J. S. et al. Soft, curved electrode systems capable of integration on the auricle as a persistent brain-computer interface. *Proc. Natl Acad. Sci. USA* **112**, 3920–3925 (2015).
111. Nicholls. B., Ang. C. S., Efstratiou C., Lee Y. & Yeo W. H. Swallowing detection for game control: using skin-like electronics to support people with dysphagia. *2017 IEEE International Conference on Pervasive Computing and Communications Workshops, PerCom Workshops 2017*. 413–418 (IEEE, 2017).
112. Lee, Y., Nicholls, B., Lee, D. S., Chen Y. & Chun Y. Soft electronics enabled ergonomic human-computer interaction for swallowing training. *Sci. Rep.* **7**, 46697 (2017).
113. Shahrim, N. A., Ahmad, Z., Wong Azman, A., Fachmi Buys, Y. & Sarifuddin, N. Mechanisms for doped PEDOT:PSS electrical conductivity improvement. *Mater. Adv.* **2**, 7118–7138 (2021).
114. Lipomi, D. J. et al. Electronic properties of transparent conductive films of PEDOT:PSS on stretchable substrates. *Chem. Mater.* **24**, 373–382 (2012).
115. Wang, Y. et al. A highly stretchable, transparent, and conductive polymer. *Sci. Adv.* **3**, 1–11 (2017).
116. Li, Y., Tanigawa, R. & Okuzaki, H. *Soft and flexible PEDOT/PSS films for applications to soft actuators.* https://doi.org/10.1088/0964-1726/23/7/074010 (2014).
117. Teo, M. Y. et al. Highly stretchable and highly conductive PEDOT: PSS/ionic liquid composite transparent electrodes for solution-processed stretchable electronics. https://doi.org/10.1021/acsami.6b11988 (2017).
118. He, H. et al. Biocompatible conductive polymers with high conductivity and high stretchability. https://doi.org/10.1021/acsami.9b07325 (2019).
119. Bates, C. M. & Bates, F. S. 50th anniversary perspective: block polymers-pure potential. https://doi.org/10.1021/acs.macromol.6b02355(2017).
120. Blau, R. et al. Intrinsically stretchable block copolymer based on PEDOT:PSS for improved performance in bioelectronic applications. *ACS Appl. Mater. Interfaces* **14**, 4823–4835 (2022).
121. Polat, B. et al. External measurement of swallowed volume during exercise enabled by stretchable derivatives of PEDOT:PSS, graphene, metallic nanoparticles, and machine learning. *Adv. Sensor Res.* **D**, 2200060 (2023).
122. Miyamoto, A. et al. Inflammation-free, gas-permeable, lightweight, stretchable on-skin electronics with nanomeshes. *Nat. Nanotechnol.* **12**, 907–913 (2017).
123. Grancarić, A. M. et al. *Conductive polymers for smart textile applications*. https://doi.org/10.1177/1528083717699368 (2018).
124. Esparza, G. L. & Lipomi D. J. Solid-phase deposition: conformal coverage. https://doi.org/10.1021/acsmaterialslett.1c00213 (2021).
125. Lipomi, D. J. et al. Skin-like pressure and strain sensors based on transparent elastic films of carbon nanotubes. *Nat. Nanotechnol.* **6**, 788–792 (2011).
126. Choudhary, K. et al. Comparison of the mechanical properties of a conjugated polymer deposited using spin coating, interfacial spreading, solution shearing, and spray coating. https://doi.org/10.1021/acsami.1c13043 (2021).
127. Jin Young, O., Kim, S., Baik, H. K. & Jeong, U. Conducting polymer dough for deformable electronics. *Adv. Mater.* **28**, 4455–4461 (2016).
128. Wessendorf, A. M. & Newman, D. J. Dynamic understanding of human-skin movement and strain-field analysis. *IEEE Trans. Biomed. Eng.* **59**, 3432–3438 (2012).
129. Obropta, E. W. & Newman, D. J. Skin strain fields at the shoulder joint for mechanical counter pressure space suit development. *IEEE Aerospace Conf. Proc.* **2016-June**, 1–9 (2016).
130. Xu, H. et al. Conductive and eco-friendly gluten/MXene composite organohydrogels for flexible, adhesive, and low-temperature tolerant epidermal strain sensors. *Colloids Surf. A Physicochem. Eng. Asp.* **636**, 128182 (2022).
131. Hamlet, S., Ezzell, G. & Aref, A. Larynx motion associated with swallowing during radiation therapy. *Int. J. Radiat. Oncol. Biol. Phys.* **28**, 467–470 (1994).
132. Amjadi, M., Kyung, K. U., Park, I. & Sitti, M. Stretchable, skin-mountable, and wearable strain sensors and their potential applications: a review. *Adv. Funct. Mater.* **26**, 1678–1698 (2016).
133. Afsarimanesh, N. et al. A review on fabrication, characterization and implementation of wearable strain sensors. *Sens. Actuators A Phys.* **315**, 112355 (2020).
134. Souri, H. et al. Wearable and stretchable strain sensors: materials, sensing mechanisms, and applications. *Adv. Intell. Syst.* **2**, 2000039 (2020).
135. Lu, Y., Biswas, M. C., Guo, Z., Jeon, J. W. & Wujcik, E. K. Recent developments in bio-monitoring via advanced polymer nanocomposite-based wearable strain sensors. *Biosens. Bioelectron.* **123**, 167–177 (2019).
136. Zhu, Y. et al. Enhanced oxidation resistance and electrical conductivity copper nanowires-graphene hybrid films for flexible strain sensors. *N. J. Chem.* **41**, 4950–4958 (2017).
137. Huang, Y. et al. Highly stretchable strain sensor based on polyurethane substrate using hydrogen bond-assisted laminated structure for monitoring of tiny human motions. *Smart Mater. Struct.* **27**. https://doi.org/10.1088/1361-665X/aaaba0 (2018).
138. Sun, X. et al. Carbon nanotubes reinforced hydrogel as flexible strain sensor with high stretchability and mechanically toughness. *Chem. Eng. J.* **382**, 122832 (2020).
139. Roh, E., Hwang, B. U., Kim, D., Kim, B. Y. & Lee, N. E. Stretchable, transparent, ultrasensitive, and patchable strain sensor for human-machine interfaces comprising a nanohybrid of carbon nanotubes and conductive elastomers. *ACS Nano* **9**, 6252–6261 (2015).
140. Hwang, B. U. et al. Transparent stretchable self-powered patchable sensor platform with ultrasensitive recognition of human activities. *ACS Nano* **9**, 8801–8810 (2015).
141. Zhang, J. et al. Highly stretchable and self-healable Mxene/polyvinyl alcohol hydrogel electrode for wearable capacitive electronic skin. *Adv. Electron. Mater.* **1900285** 1–10 (2019).
142. Zhang, S. H. et al. Wearable wide-range strain sensors based on ionic liquids and monitoring of human activities. *Sensors (Switzerland)* **17**, 1–10 (2017).
143. Wang, S. et al. Wearable stretchable dry and self-adhesive strain sensors with conformal contact to skin for high-quality motion monitoring. *Adv. Funct. Mater.* **31**. https://doi.org/10.1002/adfm.202007495 (2021).
144. Dickey, M. D. Stretchable and soft electronics using liquid metals. *Adv. Mater.* **29**, 1–19 (2017).
145. Jeong, Y. R. et al. Skin-attachable, stretchable integrated system based on liquid GaInSn for wireless human motion monitoring with multi-site sensing capabilities. *NPG Asia Mater.* **9**, 443 (2017).
146. Pan, H. & Lee, T. W. Recent progress in development of wearable pressure sensors derived from biological materials. *Adv. Healthc. Mater.* **10**, 1–17 (2021).
147. Wang, H. et al. Flexible capacitive pressure sensors for wearable electronics. *J. Mater. Chem. C Mater.* **10**, 1594–1605 (2022).

148. Chen, W. & Yan, X. Progress in achieving high-performance piezoresistive and capacitive flexible pressure sensors: a review. *J. Mater. Sci. Technol.* **43**, 175–188 (2020).
149. He, J. et al. Recent advances of wearable and flexible piezoresistivity pressure sensor devices and its future prospects. *J. Materiomics* **6**, 86–101 (2020).
150. Li, R. et al. Research progress of flexible capacitive pressure sensor for sensitivity enhancement approaches. *Sens. Actuators A Phys.* **321**, 112425 (2021).
151. Kou, H. et al. Wireless wide-range pressure sensor based on graphene/PDMS sponge for tactile monitoring. *Sci. Rep.* **9**, 1–7 (2019).
152. Xia, X., Zhang, X., Serpe, M. J. & Zhang, Q. Microgel-based devices as wearable capacitive electronic skins for monitoring cardiovascular risks. *Adv. Mater. Technol.* **5**, 1–8 (2020).
153. Maeda, M. et al. Non-invasive swallowing examination device using hetero-core fiber optic pressure sensor. *LifeTech 2021–2021 IEEE 3rd Global Conference on Life Sciences and Technologies* 315–316 (IEEE, 2021).
154. Iizuka, M. et al. A new flexible piezoelectric pressure sensor array for the non-invasive detection of laryngeal movement during swallowing. *J. Physiol. Sci.* **68**, 837–846 (2018).
155. Natta, L. et al. Conformable AlN piezoelectric sensors as a non-invasive approach for swallowing disorder assessment. *ACS Sens* **6**, 1761–1769 (2021).
156. Namasivayam-MacDonald, A. M., Barbon, C. E. A. & Steele, C. M. A review of swallow timing in the elderly. *Physiol. Behav.* **184**, 12–26 (2018).
157. Lee, J. H., Chee, P. S., Lim, E. H. & Tan C. H. Artificial intelligence-assisted throat sensor using ionic polymer–metal composite (IPMC) material. *Polymers (Basel)* **13**. https://doi.org/10.3390/polym13183041 (2021).
158. Guan, J., Zhang, D. & Li, T. Flexible pressure sensor based on molybdenum diselide/multi-walled carbon nanotubes for human motion detection. *IEEE Sens J* **21**, 10491–10497 (2021).
159. Hu, Y., Kim, E. G., Cao, G., Liu, S. & Xu, Y. Physiological acoustic sensing based on accelerometers: a survey for mobile healthcare. *Ann. Biomed. Eng.* **42**, 2264–2277 (2014).
160. Dudik, J. M., Jestrović, I., Luan, B., Coyle, J. L. & Sejdić, E. A comparative analysis of swallowing accelerometry and sounds during saliva swallows. *Biomed. Eng. Online* **14**, 1–15 (2015).
161. Khalifa, Y., Coyle, J. L. & Sejdić, E. Non-invasive identification of swallows via deep learning in high resolution cervical auscultation recordings. *Sci. Rep.* **10**, 1–13 (2020).
162. Kuramoto, N. et al. Deep learning-based swallowing monitor for realtime detection of swallow duration. *Proc. Ann. Int. Conf. IEEE Eng. Med. Biol. Soc. EMBS* **2020-July**, 4365–4368 (2020).
163. Tao, L. Q. et al. An intelligent artificial throat with sound-sensing ability based on laser induced graphene. *Nat. Commun.* **8**, 1–8 (2017).
164. Lin, J. et al. Laser-induced porous graphene films from commercial polymers. *Nat. Commun.* **5**, 5–12 (2014).
165. Cai, J., Luo, J., Wang, S. & Yang, S. Feature selection in machine learning: a new perspective. *Neurocomputing* **300**, 70–79 (2018).
166. Vaiman, M. & Eviatar, E. Surface electromyography as a screening method for evaluation of dysphagia and odynophagia. *Head Face Med* **5**, 9 (2009).
167. Ridner, S. H. et al. A prospective study of the lymphedema and fibrosis continuum in patients with head and neck cancer. *Lymphat. Res. Biol.* **14**, 198–205 (2016).
168. Macfarlane, P. W. et al. (eds.). *Comprehensive Electrocardiology* (Springer London, 2010).
169. Hymes, S. R., Strom, E. A. & Fife, C. Radiation dermatitis: clinical presentation, pathophysiology, and treatment 2006. *J. Am. Acad. Dermatol.* **54**, 28–46 (2006).
170. Kuiken*/* T. A., Lowery M. M., Stoykov N. S. The effect of subcutaneous fat on myoelectric signal amplitude and cross-talk. *Prosthet. Orthot. Int.* **27**, 48–54 (2003).
171. Selamat, N. A. & Ali, S. H. Md Automatic food intake monitoring based on chewing activity: a survey. *IEEE Access* **8**, 48846–48869 (2020).
172. Kalantarian, H., Alshurafa, N., Le, T. & Sarrafzadeh, M. Monitoring eating habits using a piezoelectric sensor-based necklace. *Comput. Biol. Med.* **58**, 46–55 (2015).
173. Chu, J. U., Moon, I., Lee, Y. J., Kim, S. K. & Mun, M. S. A supervised feature-projection-based real-time EMG pattern recognition for multifunction myoelectric hand control. *IEEE/ASME Trans. Mechatron.* **12**, 282–290 (2007).
174. Clancy, E. A., Morin, E. L., & Merletti, R.Sampling, noise-reduction and amplitude estimation issues in surface electromyography. *Ophthalmologe* **113**, 933–942 (2016).
175. Besio, G., Koka, K., Aakula, R., & Dai, W. Tri-polar concentric ring electrode development for Laplacian electroencephalography. *IEEE Trans. Biomed. Eng.* **53**, 926–933 (2006).
176. Wang, K. et al. Stretchable dry electrodes with concentric ring geometry for enhancing spatial resolution in electrophysiology. *Adv. Healthc. Mater.* **6**, https://doi.org/10.1002/adhm.201700552 (2017).
177. Garcia-Casado, J. et al. Evaluation of swallowing related muscle activity by means of concentric ring electrodes. *Sensors* **20**, 5267 (2020).
178. Park, J., You, I., Shin, S. & Jeong, U. Material approaches to stretchable strain sensors. *ChemPhysChem* **16**, 1155–1163 (2015).
179. Abu-Mahfouz, I. *Instrumentation: Theory and Practice, Part 2: Sensors and Transducers*. (Springer Nature Switzerland AG, 2022).
180. Homayounfar, S. Z. & Andrew, T. L. Wearable sensors for monitoring human motion: a review on mechanisms, materials, and challenges. *SLAS Technol* **25**, 9–24 (2020).
181. Qin, R. et al. A new strategy for the fabrication of a flexible and highly sensitive capacitive pressure sensor. *Microsyst. Nanoeng.* **7**, 1–12 (2021).
182. Ma, Z., Zhang, Y., Zhang, K., Deng, H. & Fu, Q. Recent progress in flexible capacitive sensors: Structures and properties. *Nano Mater. Sci.* https://doi.org/10.1016/j.nanoms.2021.11.002 (2022).
183. Wang, Y., Yu, Y., Wei, X. & Narita, F. Self-powered wearable piezoelectric monitoring of human motion and physiological signals for the postpandemic era: a review. *Adv. Mater. Technol.* **7**, 2200318 (2022).
184. Park, D. Y. et al. Self-powered real-time arterial pulse monitoring using ultrathin epidermal piezoelectric sensors. *Adv. Mater.* **29**. https://doi.org/10.1002/adma.201702308 (2017).
185. Ledger, D & McCaffrey, D. Inside Wearables Part 1: How Behavior Change Unlocks Long-term Engagement. *Medium* (2014).
186. Hermsen, S., Moons, J., Kerkhof, P., Wiekens, C. & De Groot, M. Determinants for sustained use of an activity tracker: observational study. *JMIR Mhealth Uhealth* **5**, e164 (2017).
187. Jung, Y. H. et al. A wireless haptic interface for programmable patterns of touch across large areas of the skin. *Nat. Electron.* **5**, 374–385 (2022).
188. Schweisfurth, M. A. et al. Feedback improves the control of prosthesis grasping force. *J. Neural. Eng.* **13**, 056010 (2016).
189. Keef, C. V. et al. Virtual texture generated using elastomeric conductive block copolymer in a wireless multimodal haptic glove. *Adv. Intell. Syst.* **2**, 2000018 (2020).
190. Lin, W. et al. Super-resolution wearable electrotactile rendering system. *Sci. Adv.* **8**. https://doi.org/10.1126/sciadv.abp8738 (2022).
191. Li, Z. et al. Air permeable vibrotactile actuators for wearable wireless haptics. *Adv. Funct. Mater.* **33**, 2211146 (2023).
192. Yin, J., Hinchet, R., Shea, H. & Majidi, C. Wearable soft technologies for haptic sensing and feedback. *Adv. Funct. Mater.* **31**, 2007428 (2021).
193. Yu, X. et al. Skin-integrated wireless haptic interfaces for virtual and augmented reality. *Nature* **575**, 473–479 (2019).
194. Moroni, M., Servin-Vences, M. R., Fleischer, R., Sánchez-Carranza, O. & Lewin, G. R. Voltage gating of mechanosensitive PIEZO channels. *Nat. Commun.* **9**, 1096 (2018).
195. McNeal, D. R. Analysis of a model for excitation of myelinated nerve. *IEEE Trans. Biomed. Eng.* **BME-23**, 329–337 (1976).
196. Kajimoto, H., Kawakami, N., Tachi, S. & Inami, M. SmartTouch: electric skin to touch the untouchable. *IEEE Comput. Graph. Appl.* **24**, 36–43 (2004).
197. Kourtesis, P., Argelaguet, F., Vizcay, S., Marchal, M. & Pacchierotti, C. Electrotactile feedback applications for hand and arm interactions: a systematic review, meta-analysis, and future directions. *IEEE Trans. Haptics* **15**, 479–496 (2022).
198. Zhu, J. et al. Improving compliance with swallowing exercise to decrease radiotherapy-related dysphagia in patients with head and neck cancer. *Asia Pac. J. Oncol. Nurs.* **10**, 100169 (2023).
199. O'Brien, M. K. et al. Advanced machine learning tools to monitor biomarkers of dysphagia: a wearable sensor proof-of-concept study. *Digit. Biomark.* **5**, 167–175 (2021).
200. Liu, S., Rao, Y., Jang, H., Tan, P. & Lu, N. Strategies for body-conformable electronics. *Matter* **5**, 1104–1136 (2022).
201. Yang, Y. et al. Wireless multilateral devices for optogenetic studies of individual and social behaviors. *Nat. Neurosci.* **24**, 1035–1045 (2021).
202. Nan, K. et al. Mucosa-interfacing electronics. *Nat. Rev. Mater.* **7**, 908–925 (2022).
203. Chen, J. C. et al. A wireless millimetric magnetoelectric implant for the endovascular stimulation of peripheral nerves. *Nat. Biomed. Eng.* **6**, 706–716 (2022).
204. Sayeed, S. Y. B. et al. Chipscale piezo-magnetostrictive interfaces—a new simplified and microminiaturized telemetry paradigm for medical device packages. In: *2021 IEEE 71st Electronic Components and Technology Conference (ECTC)*. 1219–1225 (IEEE, 2021).

ACKNOWLEDGEMENTS

This work was supported by the National Science Foundation award CBET-2223566 and a gift from PepsiCo & the Gatorade Sports Sciences Institute. Additional support was provided by the member companies of the Center for Wearable Sensors in the

Jacobs School of Engineering at the University of California, San Diego, including Dexcom, Gore, Honda, Huami, Instrumentation Laboratory, Kureha, Merck KGaA, PepsiCo, Roche, Samsung, and Sony. This work was performed in part at the San Diego Nanotechnology Infrastructure (SDNI), a member of the National Nanotechnology Coordinated Infrastructure, which is supported by the National Science Foundation (Grant ECCS-1542148). A.A. acknowledges the support of the Kuwait Foundation for the Advancement of Sciences (KFAS). Figures 1a, 2a, 3a were partially generated using BioRender resources.

AUTHOR CONTRIBUTIONS

The authors' contributions to this review are as follows: Initial conception: B.P., D.L. Guidance: D.L., E.H.S., K.A.H. Literature search and assembly: T.R., B.P., A.A. Writing: T.R., A.A., B.P., D.J.L. Figures and table: T.R., B.P. Editing: T.R., D.J.L., E.H.S., K.A.H., A.A.

COMPETING INTERESTS

The authors declare no competing interests.

ADDITIONAL INFORMATION

Correspondence and requests for materials should be addressed to Darren J. Lipomi.

Reprints and permission information is available at http://www.nature.com/reprints

Publisher's note Springer Nature remains neutral with regard to jurisdictional claims in published maps and institutional affiliations.